

THE ANALYSIS OF SUCKER-ROD PUMPING INSTALLATIONS

6

CHAPTER OUTLINE

6.1	Introduction	424
6.2	Well Testing.....	424
6.2.1	Production Testing	425
6.2.1.1	Conventional production tests.....	425
6.2.1.2	Inferred production calculations	425
6.2.2	Determination of Annular Liquid Levels.....	427
6.2.2.1	Acoustic surveys	427
6.2.2.2	Calculation of liquid levels	429
6.2.3	Bottomhole Pressure Calculations.....	434
6.2.3.1	Early methods.....	434
6.2.3.2	Static conditions.....	437
6.2.3.3	Flowing conditions	440
6.2.4	Determination of Well Inflow Performance	445
6.3	Dynamometer Surveys.....	448
6.3.1	Basic Dynamometer Types	448
6.3.1.1	Polished rod dynamometers	448
6.3.1.2	Downhole dynagraphs.....	452
6.3.2	The Use of Conventional Dynamometers	453
6.3.2.1	Recording a dynamometer card.....	453
6.3.2.2	Checking the condition of pump valves.....	454
6.3.2.3	Measuring the counterbalance effect	457
6.3.3	The Use of Electronic Dynamometers	458
6.3.3.1	Introduction	458
6.3.3.2	Recording a representative card	460
6.3.3.3	Checking the condition of pump valves.....	460
6.3.3.4	Counterbalance effect measurement	464
6.4	Interpretation of Dynamometer Cards	465
6.4.1	Conventional Dynamometer Cards	466
6.4.1.1	Basic loads	468
6.4.1.2	Polished rod horsepower	469

6.4.2 Cards from Electronic Dynamometers.....	471
6.4.2.1 <i>Ideal pump cards</i>	471
6.4.2.2 <i>Basic analysis</i>	475
6.4.2.3 <i>Detection of common pump problems</i>	479
6.4.2.4 <i>Pump intake pressure calculations</i>	495
6.4.3 Modern Interpretation Methods.....	499
References	500

6.1 INTRODUCTION

This chapter deals with the methods and procedures that are available to **analyze** the operation of sucker-rod pumping wells. The first broad topic discussed covers the **inflow** performance testing of wells placed on rod pumping. As discussed in this chapter, special **well testing** procedures are required to conduct a production test because the methods developed for flowing or gas-lifted wells are not applicable. Among these, the **acoustic** determination of annular liquid levels is described, since such measurements form the basis of most of the testing procedures. The results of a properly conducted well test provide valuable information on actual well **potential** and help the pumping analyst to decide on possible changes to the pumping system.

The most common procedures to measure and analyze the operating conditions of rod-pumping installations use polished rod **dynamometers**; this chapter discusses the **hardware** used and the **procedures** followed when making dynamometer surveys. The use of hydraulic and electronic dynamometers to take surface dynamometer cards as well as to test the downhole pump's valves is detailed. Interpretation of surface and downhole dynamometer cards is also presented, with an emphasis on the evaluation of **pump cards** calculated from surface data using the solution of the damped wave equation.

6.2 WELL TESTING

The purpose of well testing is the determination of the well's **inflow performance** behavior. This involves the measurement of production rates for **several** bottomhole pressures and the construction of the well's inflow performance relationship (**IPR**) curve. Since the performance of any producing well constantly changes with the **depletion** of the reservoir and with other factors, wells must be tested **regularly** for changes in their inflow performance. In case of flowing and gas-lifted oil wells, an inflow performance test is conducted by running a pressure element (pressure bomb) to the bottom inside the tubing string and thereby recording flowing and static bottomhole pressures. This procedure cannot be applied to rod-pumped wells because the rod string present in the tubing prevents the running of wireline tools in the well. Thus the well must be **killed** and the rods pulled out before a downhole pressure survey can be conducted involving high workover costs, which are usually prohibitive. Although theoretically possible, pressure measurements in the well annulus are also ruled out as a result of many practical implications, such as restricted passage area in the annulus, a high probability of wireline breaks, etc. Therefore, the inherent need for running inflow performance tests also in rod-pumped wells necessitated the development of techniques and procedures different from those applied in wells placed on any other type of lift.

6.2.1 PRODUCTION TESTING

6.2.1.1 Conventional production tests

As discussed before, knowledge of the well's **liquid rate** is absolutely necessary to estimate its inflow performance during well testing. A production test, a standard part of oil field operations, supplies the liquid and gas production **rates** obtained from the well through periodic **measurements**. Liquid rates are conventionally measured in **storage tanks** by gauging; modern field management utilizes **lease automatic custody transfer** (LACT) units for this purpose. The liquid rates obtained by a production test are used for several reasons: to fulfill regulatory obligations, to facilitate reserve estimations, to help reservoir management, etc. Since wells are tested only **periodically**, production rates between tests are assumed to be unchanged; this is the basis of production allocation between several wells.

In order to establish an accurate IPR curve the production rate used in well testing must come from the **latest** production test, but for best results **simultaneous** measurements of the production rate and the flowing bottomhole pressure are recommended.

6.2.1.2 Inferred production calculations

Conventional well tests have an inherent **inaccuracy** due to the errors in liquid rates because these rates are measured only **periodically**. The concept of **inferred** production rates [1–3] eliminates this problem and uses the downhole pump as a **metering** device to calculate the pump's liquid and gas production rate for **every** pumping cycle. Cycle volumes accumulated for 24 h indicate the well's daily production rate, which is a very accurate estimation of the actual rate obtained from the well. This novel technique requires the continuous calculation of **downhole** pump cards from surface dynamometer data, which some of the advanced pump-off controller (**POC**) devices are capable to accomplish. The use of inferred production, if applied in sucker-rod pumped fields, may **reduce** or completely **eliminate** traditional production testing procedures and the need for related facilities.

The **background** of inferred production rate calculations is very simple: if the **effective** plunger stroke length used for liquid production is known, then the liquid volume passing through the pump during a pumping cycle is equal to the product of the plunger's cross-sectional area and the effective stroke length. In any consistent units this is written as:

$$\Delta V = A_p S_{\text{eff}} \quad (6.1)$$

where:

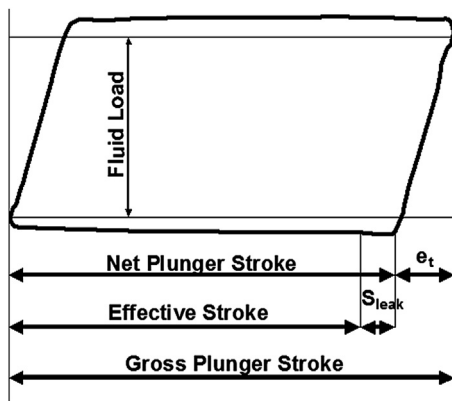
ΔV = liquid volume per pumping cycle,

A_p = plunger area, and

S_{eff} = effective stroke length.

The only unknown in the formula is the **effective** plunger stroke; this must be **estimated** from the pump card, which, in turn, is calculated from the measured surface dynamometer card using the damped wave equation. In case a negligible gas rate flows through the pump, the **effective** plunger stroke is found by reducing the gross plunger stroke length by the following items, read from the pump card (see Fig. 6.1):

- Tubing stretch, e_t , calculated from **Hooke's law** using the fluid load. This term is zero if the tubing is anchored.
- Stroke loss, S_{leak} , due to fluid **leakage** through the pump. This parameter is determined from the actual leakage rate in the pump, the cross-sectional area of the plunger, and the pumping speed.

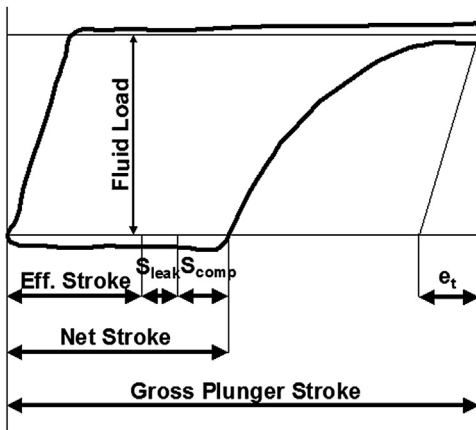
**FIGURE 6.1**

Schematic pump card in a well with negligible gas production.

Plunger leakage is usually calculated from the evaluation of the loads and velocities of the plunger or found from the data of valve tests.

If there is a considerable amount of **free gas** passing through the pump, the effective stroke needed for inferred production calculations is based on the **net** stroke. This, in turn, is determined from the shape of the pump card, as shown in Fig. 6.2. The **effective** stroke length used for liquid production is less than the net stroke; the difference is the **sum** of the following terms:

- Stroke loss, s_{leak} , due to fluid **leakage** through the pump; calculated as before.
- Stroke loss, s_{comp} , to compensate for the **compression** of free gas that enters the pump while the standing valve is open. Determination of the stroke loss due to gas compression requires complex calculations.

**FIGURE 6.2**

Schematic pump card in a well with considerable free gas production.

In any case (with or without considerable gas production) the **in situ** liquid volume passing through the pump is simply found from the **effective** plunger stroke length and the plunger cross-sectional **area**; see Eq. (6.1). Since inflow performance calculations require production rates to be expressed in standard units, the *in situ* volumes must be corrected by the appropriate **volume factors** to get stock-tank barrels.

As detailed previously, utilization of inferred production rates involves quite **complex** calculations; these have to be preprogrammed in the memory of the surface control device installed on the wellhead. Up-to-date POC devices usually include the necessary instrumentation and provide continuous information on the well's production rates, thus facilitating well testing with a high accuracy; they can even replace conventional testing procedures. The **accuracy** of inferred production (IP) calculations was compared to stock-tank volume measurements for three wells and the difference was found to be less than 2% [2]. A different source [4] reported similar accuracies for a case of 15 wells; inferred production rate calculations can thus provide a reliable alternative to conventional well testing.

6.2.2 DETERMINATION OF ANNULAR LIQUID LEVELS

As mentioned previously, a **packer** is not commonly run in a rod-pumped well; thus, well fluids may freely enter the casing–tubing annulus. It was also shown that the **height** above the formation of the fluid column is a direct indicator of the well's actual **bottomhole** pressure. This fact is utilized in most of the well testing procedures developed for pumping wells, which rely on the measurement of annular liquid **levels**. After the annular liquid level is known, static and flowing **bottomhole pressures** can be found by calculation. In the following, the determination of annular liquid levels is discussed first, and then the available calculation models are detailed that permit the calculation of bottomhole pressures.

6.2.2.1 Acoustic surveys

The most common method of finding the liquid level in a pumping well's annulus is by conducting an acoustic well survey, also called **well sounding**. This survey operates on the principles of propagation and reflection of **pressure waves** in gases. Using a wave source, a pressure **pulse** (usually an acoustic impulse) is produced at the surface in the casing–tubing annulus, which travels in the form of pressure **waves** along the length of the annular gas column. These pressure waves are **reflected** (echoed) from every depth where a change of cross-sectional area occurs, caused by tubing collars, casing liners, well fluids, etc. The reflected waves are picked up and converted to electrical signals by a **microphone**, also placed at the surface, and **recorded** on paper or by electronic means. An evaluation of the reflected signals allows the determination of the depth to the liquid level in the well.

The acoustical well sounder consists of two basic components: the wellhead assembly and the recording and processing unit. The wellhead assembly is easily connected to the casing annulus by means of a threaded nipple. It contains a mechanism that **creates** the sound wave and a **microphone** that picks up the signals. Conventional well sounders utilize blank **cartridges** with black powder, which are fired either manually or by remote control. Modern well sounder units employ so-called **gas guns**, which provide the required pressure impulse by suddenly **discharging** a small amount of high-pressure gas (CO_2 or N_2) into the annulus. The recording unit processes the electric signals created by the microphone, by filtering and amplification. The processed signals are then **recorded**

on a chart recorder in the function of time. The depth of the liquid level in the annulus is found by the proper **interpretation** of the acoustic chart.

An example acoustic chart is given in Fig. 6.3, which shows analog recordings of reflected sound signals on a **strip chart**. As seen, every tubing **collar** is identified by a local **peak** of the signal, whereas the liquid level is clearly marked by a much larger reflection. Determination of the liquid level depth is possible by either counting the number of **collar signals** and comparing these data to well records or finding the reflection **time** from the liquid level [5,6]. Time readings are made possible with the use of 1-s timing signals that are also recorded on the chart. If reflection time and the acoustic velocity are known, then liquid level **depth** is found from the formula given below:

$$L = \frac{\Delta t v_s}{2} \quad (6.2)$$

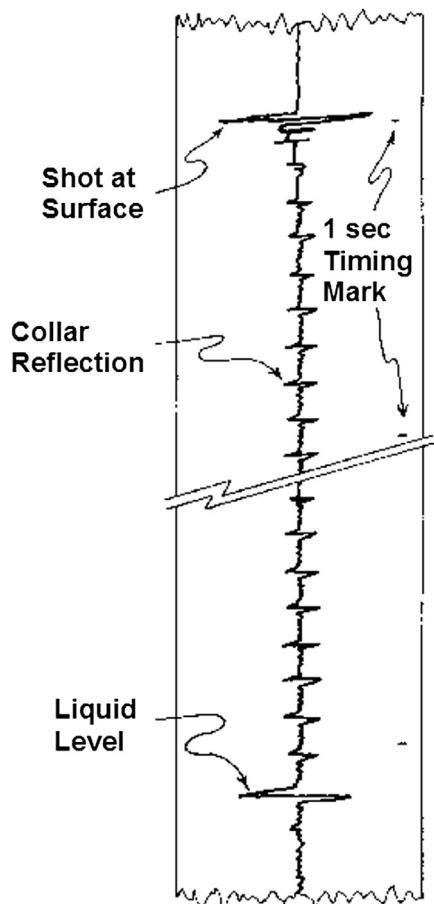


FIGURE 6.3

An example strip-chart recording from an acoustic survey.

where:

- L = depth to liquid level from surface, ft,
- Δt = time between generation and reflection, s, and
- v_s = acoustic velocity in the gas, ft/s.

The accuracy of acoustic liquid level surveys is highly dependent on an accurate knowledge of the **acoustic velocity** valid under the actual conditions. The use of some form of the **equation of state** for the gas can supply these values [7]. In wells with **uniform** gas composition in the casing annulus, reliable acoustic velocities are calculated from this approach. The majority of wells that **vent** annulus gas to the flowline contain uniform gas columns.

The casing annulus of wells not venting gas or shut in for longer periods usually contains a gas column whose composition **varies** with depth. In such cases, great discrepancies in local acoustic velocities may occur and special precautions are necessary.

The advantages of acoustic well surveys over the **direct** determination of bottomhole pressures are the much smaller **costs** involved, the elimination of well **killing** and workover operations, and the reduced time requirement. Therefore, acoustic surveys are widely used in rod-pumping analysis. However, in case the annular fluid has a high tendency to **foam**, no firm signals on the liquid level can be attained. The latest developments in acoustic survey techniques include the automatic liquid level **monitor** [8], which automatically runs acoustic surveys and can also conduct pressure buildup and drawdown tests on pumping wells. Modern acoustic units employ microcomputers and advanced digital data acquisition techniques and ensure high accuracy and reliability of liquid level determinations [9–12].

6.2.2.2 Calculation of liquid levels

Instead of directly **measuring** liquid levels, the procedure proposed by **Alexander** [13,14] allows the indirect determination of the actual liquid level in pumping wells with a sufficient gas production. His method is based on a **mass balance** equation written on the gas volume contained in the casing–tubing annulus (see Fig. 6.4). In steady-state normal operations, the gas rate **entering** the annulus from the formation, q_1 , equals the rate of gas **vented** into the flowline, q_2 . Thus a constant gas volume of V is maintained in the annulus above the liquid level. If either of the gas volumetric **rates** will change, a corresponding change in the annular **volume** will occur. This phenomenon is easily described, if a mass **balance** is written on the annular gas, by equating the mass rates flowing **in** and **out** of the system with the change in the system's mass:

$$q_{m1} - q_{m2} = \frac{d}{dt} m \quad (6.3)$$

where:

- q_{m1} = mass rate of annular gas influx, lb/min,
- q_{m2} = mass rate of gas leaving the annulus, lb/min, and
- m = mass of gas contained in the annulus, lb.
- t = time, min

Mass flow rates are expressed with the **volumetric** gas flow rates, using the **engineering equation of state**:

$$q_m = q \frac{P_{sc} M}{R T_{sc}} \quad (6.4)$$

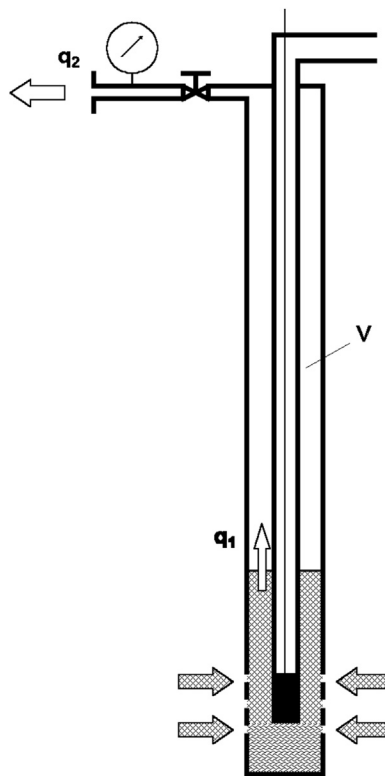
**FIGURE 6.4**

Illustration for writing up the mass balance equation for the annular gas volume of a pumping well.

where:

q_m = mass flow rate, lb/min,

q = volumetric flow rate at standard conditions, cu ft/min,

p_{sc} = standard pressure, 14.65 psia,

M = molecular weight of the gas, lb/mole,

T_{sc} = standard temperature, 520° Rankine, and

R = universal gas constant.

The system's mass is found from the **engineering equation of state** as:

$$m = \frac{pVM}{RTZ} \quad (6.5)$$

where the parameters not defined above are:

m = mass of gas, lb,

p = pressure, psia,

V = annular gas volume, cu ft,

T = absolute temperature, degrees Rankine, and

Z = gas deviation factor, -.

In order to find the final form of the basic equation (Eq. 6.3), the simplifying **assumption** is made that gas temperature, T , and deviation factor, Z , are **independent** of time. Then, after substitution of Eq. (6.4) into the basic equation and after differentiation of Eq. (6.5), we get:

$$q_1 - q_2 = \frac{50.8}{TZ} \left(V \frac{dp}{dt} + p \frac{dV}{dt} \right) \quad (6.6)$$

where:

q_1, q_2 = gas volumetric rates, Mscf/d,

p = pressure, psia,

V = annular gas volume, cu ft,

T = absolute temperature, degrees Rankine, and

Z = gas deviation factor, –.

Alexander uses this mass balance equation to find the annular liquid **level** for two basic physical models. The constant **volume** model assumes that casing gas volume does not considerably change during short shut-in periods when the surface casing valve is closed. The constant bottomhole **pressure** model, on the other hand, accounts for changes in annular gas volume but assumes a constant bottomhole pressure to persist during short-time fluid level buildup periods. Both models are used with the following experimental procedure illustrated in Fig. 6.4.

First, the casing **wing** valve at the surface is **closed**, which entails a gradual increase in casinghead pressure due to the continuous inflow of gas, q_1 , from the formation into the annulus. The **pressure buildup** is recorded with a high-precision device, a dead-weight tester or an electronic transducer. Usually, a 5 psia pressure **increase** or a 10-min testing **period** is employed to ensure a negligibly small change in annular liquid level. Then, the casing valve is **opened** and gas is bled from the annulus at a measured rate. A critical flow **prover** provides an ideal tool for this purpose. During the venting period, casinghead pressure continuously changes because gas is removed from the system. Again, changes in casinghead pressure are **measured** and recorded with high accuracy. The test just described can be accomplished with the pumping unit either in **operation** or **shut down**, and the formulae detailed below are utilized to find the required parameters.

Using the constant casing **volume** approach, the change in casing volume is assumed to be negligible, i.e., dV/dt is zero in Eq. (6.6). Now, if the casing valve is closed, gas volumetric rate q_2 equals zero because no gas is vented from the annulus, and the basic equation is solved for the annular gas inflow rate, q_1 :

$$q_1 = \frac{50.8}{TZ} V \left(\frac{dp}{dt} \right)_1 \quad (6.7)$$

where:

q_1 = annular gas flow rate, cu ft/d, and

$(dp/dt)_1$ = pressure buildup rate during casing valve shut-off, psia/min.

The next step of the experimental procedure involves the measurement of the gas **rate**, q_2 , through the critical flow prover, after the casing valve has been opened. The basic equation for these conditions is written as:

$$q_1 - q_2 = \frac{50.8}{TZ} V \left(\frac{dp}{dt} \right)_2 \quad (6.8)$$

where: $(dp/dt)_2$ = pressure change rate during gas bleed-down from the casing, psia/min.

Equations (6.7) and (6.8) contain two **unknowns** and can simultaneously be solved for those parameters:

$$V = \frac{q_2 TZ}{50.8[(dp/dt)_1 - (dp/dt)_2]} \quad (6.9)$$

$$q_1 = q_2 \frac{(dp/dt)_1}{(dp/dt)_1 - (dp/dt)_2} \quad (6.10)$$

where:

V = volume of gas contained in the annulus, cu ft,

q_2 = gas vent rate from annulus, Mscf/d,

T = average absolute temperature of annulus gas, degrees Rankine,

Z = average gas deviation factor in annulus, –,

q_1 = annular gas flow rate, Mscf/d,

$(dp/dt)_1$ = time rate of change of casinghead pressure during casing shut-in, psia/min, and

$(dp/dt)_2$ = time rate of change of casinghead pressure during casing vent period, psia/min.

Since the annular gas volume, V , is calculated with **average** pressure and temperature in the above formulae, a **correction** is necessary if surface pressure data are used. Based on the **engineering equation of state**, the corrected volume is found from the value just calculated:

$$V_{\text{corrected}} = V \frac{p_{\text{surf}}}{p_{\text{avg}}} \quad (6.11)$$

The pressure ratio in the above formula is derived from the equation used to calculate the pressure distribution in a static gas column:

$$\frac{p_{\text{surf}}}{p_{\text{avg}}} = \frac{L \left[0.001877 \frac{SpGr}{T_{\text{avg}} Z_{\text{avg}}} \right]}{\exp \left[0.001877 L \frac{SpGr}{T_{\text{avg}} Z_{\text{avg}}} \right] - 1} \quad (6.12)$$

where:

p_{surf} , p_{avg} = surface and average gas pressure, respectively, psi,

L = uncorrected depth to liquid level, ft,

$SpGr$ = gas specific gravity, –,

T_{avg} = average absolute temperature of gas column, degrees Rankine, and

Z_{avg} = gas deviation factor at average conditions, –.

It can be shown [13,14] that the constant bottomhole pressure model results in calculated gas volumes **smaller** than those received from the constant volume model. The relationship of the two gas volumes is given below:

$$V' = V - 5.61p \frac{C}{grad} \quad (6.13)$$

where:

V' = annular gas volume from the constant bottomhole pressure model, cu ft,

V = annular gas volume from the constant volume model, cu ft,

p = surface pressure, psia,

$grad$ = hydrostatic gradient in the liquid column, psi/ft, and
 C = capacity of the annulus, bbl/ft.

The depth of the liquid **level** from the surface equals the length of the gas **column**, which, in turn, is found from the calculated annular gas volume and the capacity of the annulus:

$$L = \frac{V}{5.61C} \quad (6.14)$$

where:

L = depth of the liquid level, ft,
 V = annular gas volume, cu ft, and
 C = annular capacity, bbl/ft.

In conclusion, **Alexander's** method discussed above allows the calculation of liquid level depths in pumping wells by following a simple testing procedure. A similar calculation model was developed by **Hasan and Kabir** [15].

EXAMPLE 6.1: FIND THE DYNAMIC LIQUID LEVEL IN THE ANNULUS WITH ALEXANDER'S PROCEDURE, FOR THE FOLLOWING CONDITIONS:

Depth of perforations = 5,000 ft
Pump setting depth = 5,000 ft
Annular capacity = 0.019 bbl/ft
Average annulus temperature = 70 F
Average deviation factor in annulus = 0.89
Gas specific gravity = 0.78
Oil gradient = 0.3 psi/ft
Surface casing pressure = 40 psi
 $(dp/dt)_1 = 0.05$ psi/min
 $(dp/dt)_2 = -0.1$ psi/min
Casing gas vent rate = 4.0 Mscf/d

Solution

First, the constant pressure model is used to calculate annular gas volume, using [Eq. \(6.9\)](#):

$$V = [4(70 + 460)0.89]/[50.8(0.05 + 0.1)] = 1,886.8/7.62 = 248 \text{ cu ft.}$$

The liquid level depth is found from [Eq. \(6.14\)](#):

$$L = 248/(5.61 \times 0.019) = 2,327 \text{ ft.}$$

The pressure correction factor is calculated from [Eq. \(6.12\)](#):

$$\begin{aligned} p_{\text{surf}}/p_{\text{avg}} &= 2,327[0.001877 \times 0.78/(70 + 460)/0.89]/\{\exp[0.001877 \times 2,327 \times 0.78/(70 + 460)/0.89] - 1\} \\ &= 0.00722/0.00725 = 0.996. \end{aligned}$$

Corrected gas volume is by [Eq. \(6.11\)](#):

$$V_{\text{corrected}} = 248 \times 0.996 = 247 \text{ cu ft.}$$

The corrected fluid level is thus:

$$L = 247/5.61/0.019 = 2,317 \text{ ft.}$$

Now the constant bottomhole pressure model is used to calculate the gas volume, and Eq. (6.13) gives:

$$V' = 247 - 5.61 \times 40 \times 0.019 / 0.30 = 247 - 14 = 233 \text{ cu ft.}$$

Use Eq. (6.14) to find the liquid level corresponding to this gas volume:

$$L = 233 / 5.61 / 0.019 = 2,186 \text{ ft.}$$

In conclusion, the actual liquid level is expected to lie between 2,186 and 2,317 ft.

6.2.3 BOTTOMHOLE PRESSURE CALCULATIONS

6.2.3.1 Early methods

This section briefly discusses the bottomhole pressure determination methods developed in **early** production practice. The accuracies to be expected from these procedures can be substantially **lower** than those achieved with the more modern approaches detailed later.

6.2.3.1.1 Walker's method

Walker's well testing method [16] (see also Nind [17]), is based on the following theoretical considerations. Under steady-state conditions, i.e., pumping a **constant** liquid rate, the pumping well's flowing bottomhole pressure is **independent** of the actual depth of the liquid level in the casing annulus. This is easy to see because a constant liquid removal from a well means a stable pressure at the bottom. Since the annulus is directly connected to the pump intake (no packer is present), the pressure at the bottom of the annular gaseous fluid column should be equal to the well's bottomhole pressure. However, annulus pressure at that depth is the sum of three components: surface pressure and the pressures of the gas and fluid columns that exist above the formation. Therefore, the **same** bottomhole pressure can exist with a **shorter** fluid column if surface gas pressure plus gas column weight is greater, and vice versa.

Figure 6.5 illustrates the basics of **Walker's method**. At the beginning, the well is pumped **normally** and the surface casinghead pressure, p_{c1} , is noted. At the same time, the stabilized fluid column **height** above the formation, h_1 , is measured via an acoustic **survey**. Then, by the use of a pressure regulator on the surface, casinghead pressure is **increased** to a higher value, p_{c2} . After a sufficiently long pumping period to reach **stabilized** conditions, the depressed liquid **level** is measured, and the new fluid column height, h_2 , is calculated. According to the above considerations, the **pressure** at formation depth is the **same** for the two cases and can be written as follows:

$$p_{wf} = p_{c1} + p_{g1} + h_1 grad \quad (6.15)$$

$$p_{wf} = p_{c2} + p_{g2} + h_2 grad \quad (6.16)$$

where:

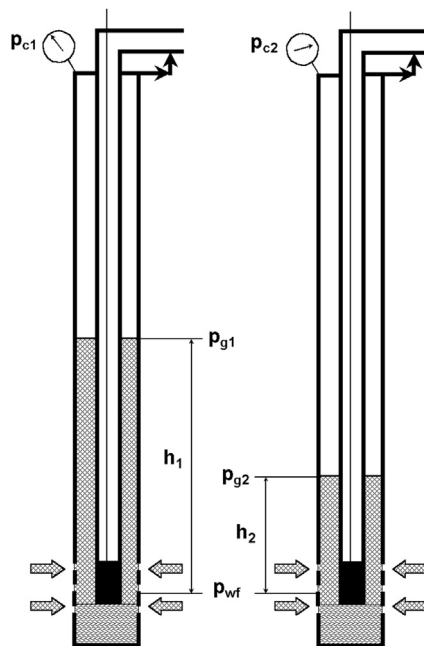
p_{wf} = flowing bottomhole pressure, psi,

p_{c1}, p_{c2} = casinghead pressures in the two cases, psi,

p_{g1}, p_{g2} = gas column pressures in the two cases, psi,

h_1, h_2 = fluid column heights above the formation in the two cases, ft, and

$grad$ = hydrostatic gradient of the gaseous fluid column in the annulus, psi/ft.

**FIGURE 6.5**

Walker's method for determining the flowing bottomhole pressure in a pumping well.

It can be shown that the implied **assumption** of a constant fluid gradient, $grad$, in the two cases is **justified**, and the above two equations can simultaneously be solved for the two unknowns: the fluid gradient and bottomhole pressure. Fluid gradient is found from the formula:

$$grad = \frac{(p_{c2} + p_{g2}) - (p_{c1} + p_{g1})}{h_1 - h_2} \quad (6.17)$$

Flowing bottomhole pressure, p_{wf} , is then calculated from either of the two equations given above (Eq. (6.15) or (6.16)).

Since **Walker's method** is only valid for **stabilized conditions**, great care must be taken to reach steady-state fluid **levels** in both tests. Since this process can take considerable time, sometimes even several days, the use of this bottomhole pressure determination method is limited.

EXAMPLE 6.2: CALCULATE THE FLOWING BOTTOMHOLE PRESSURE WITH WALKER'S METHOD IN A WELL WITH THE FOLLOWING DATA:

Depth of perforations = 4,000 ft

Pump setting depth = 4,000 ft

Gas specific gravity = 0.8

Measured acoustic liquid levels and casinghead pressures are:

	First Case	Second Case
Acoustic level, ft	2,000	3,600
Casing pressure, psi	200	490

Solution

The fluid column heights above the formation for the two cases (see Fig. 6.5) are:

$$h_1 = 4,000 - 2,000 = 2,000 \text{ ft.}$$

$$h_2 = 4,000 - 3,600 = 400 \text{ ft.}$$

The pressure at the bottom of the gas column is calculated from gas gradient curves, resulting in pressure gradients of 6 psi/1,000 ft and 16 psi/1,000 ft, for casinghead pressures of 200 psi and 490 psi, respectively. Gas column pressures are thus:

$$p_{g1} = 2,000 \times 6/1,000 = 12 \text{ psi.}$$

$$p_{g2} = 3,600 \times 16/1,000 = 58 \text{ psi.}$$

The average fluid gradient in the annulus is found from Eq. (6.17):

$$\text{grad} = [(490 + 58) - (200 + 12)]/[2,000 - 400] = 336/1,600 = 0.21 \text{ psi/ft.}$$

Flowing bottomhole pressure can now be calculated by Eq. (6.15):

$$p_{wf} = 200 + 12 + 2,000 \times 0.21 = 632 \text{ psi.}$$

A check is made in the second case, using Eq. (6.16):

$$p_{wf} = 490 + 58 + 400 \times 0.21 = 632 \text{ psi.}$$

As expected, the two flowing bottomhole pressures are equal.

6.2.3.1.2 Other methods

Agnew [18,19] proposed an **approximate** calculation model based on dynamometer measurements. He utilized the data of the well-known standing and traveling valve **tests** to arrive at an approximate bottomhole pressure. The accuracy of the procedure is highly dependent on the proper execution of these tests and also can be affected by downhole problems such as excessive friction, which considerably change measured rod loads.

One old practical method is the so-called **gas blow-around method**, which can be applied in wells with **considerable** gas production. Its principle is that if the fluid level is **depressed** to the pump setting depth, then pump intake pressure is found from the hydrostatic pressure of the gas **column**. Since the **length** of the gas column is precisely known (it is at pump level), its pressure can be calculated very accurately. The inaccuracies of bottomhole pressure calculations, introduced by errors in fluid **level** and fluid **gradient** values, are thus eliminated. The testing procedure requires the use of a pressure regulator and a dynamometer at the surface. The casing pressure is **increased** with the regulator until gas is **blown** around from the annulus into the pump. This occurs when the dynamometer card shows typical gas interference symptoms. The main drawback of this procedure is the usually long time required for **stabilized** conditions to occur [20].

6.2.3.2 Static conditions

If a pumping well is **shut in** for a sufficient period of time, i.e., the pumping unit is stopped and the casing valve is closed, then stabilized conditions in the well will occur. Gas, if produced from the reservoir, **accumulates** in the upper portion of the casing annulus, and liquid **fills** up the lower part of it. The well develops its static bottomhole pressure (SBHP) at the formation, which pressure balances the combined hydrostatic pressures of the liquid and gas **columns**. Therefore, static bottomhole pressure is easily found by adding to the casinghead pressure, measured at the surface, the pressures exerted by these columns, as given below:

$$p_{ws} = p_c + p_g + p_l \quad (6.18)$$

where:

p_{ws} = static bottomhole pressure (SBHP), psi,

p_c = casinghead pressure, psi,

p_g = hydrostatic pressure of the annular gas column, psi, and

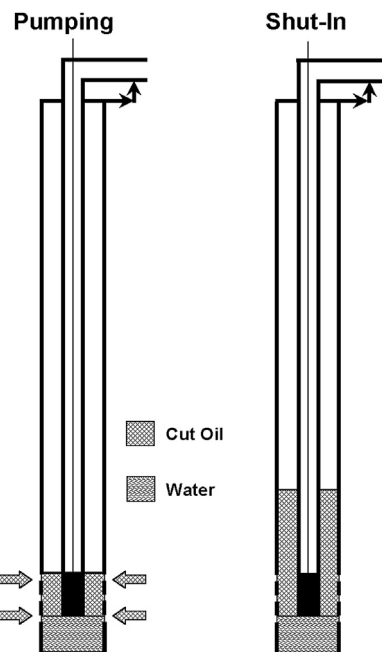
p_l = hydrostatic pressure of the annular liquid column, psi.

Surface casing pressure, p_c , is measured with a **high-precision** pressure gauge or a dead-weight tester. Accurate measurements are **required** since, in most cases, this component accounts for a large part of the final bottomhole pressure. The hydrostatic pressure in the gas **column**, p_g , can only be determined if the **depth** to the static liquid level in the well is known, usually found from an **acoustic** survey. A proper evaluation of this pressure must account for gas composition and temperature distribution in the annulus and involves an iterative calculation procedure. For approximate calculations the universal gas gradient chart developed in Fig. 2.9 can be used; the chart is reproduced in **Appendix A**.

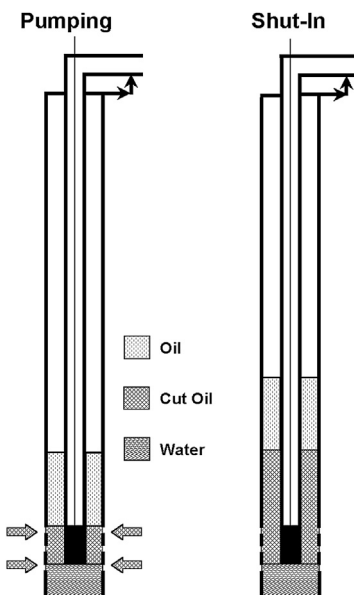
The last component of the bottomhole pressure, the liquid column's **hydrostatic** pressure, p_l , is mainly governed by the hydrostatic gradient of the annular liquid. Determination of this gradient poses no problems if **pure** oil is produced, but water-cut oil production needs special considerations. As shown by McCoy et al. [21], the **composition** of the annular liquid column depends on the relation of the dynamic liquid level to pump setting depth, valid just **before** the well was shut down. A general rule is that in steady-state pumping conditions, due to gravitational **separation** of the oil from the water, all liquid above the pump is **pure oil**. After the well is shut down, a water-cut liquid with approximately the same water–oil ratio (WOR), as measured in a test separator, flows below the oil column.

Figures 6.6 and 6.7 show the pumping and shut-in conditions in the annulus when the pump is set at the depth of the **formation**. If, during pumping, the stabilized liquid level is at the pump **intake**, then after shut-in, all liquid above the formation will be with the same WOR as found in a previous production test (Fig. 6.6). Although this liquid column will, with time, separate into **separate** water and oil sections, its hydrostatic **pressure** does not change. On the other hand, if the dynamic liquid level is above the pump before shut-in, the liquid column contains **only oil**. As seen in Fig. 6.7, this oil column remains on the top of the water-cut liquid after the well is shut down. Figures 6.8 and 6.9 illustrate the same pumping and static conditions for wells that have the pump run above the depth of the perforations.

After the WOR **distribution** in the liquid column has been established, the hydrostatic pressure is calculated with the help of static **gradients** for the water and the oil. For approximate calculations, average gradients taken at an average column temperature and pressure may be used. More accurate bottomhole pressure predictions require **step-wise** calculations when the effects of actual pressure and temperature on oil and water densities can properly be accounted for [21].

**FIGURE 6.6**

Pumping and shut-in conditions in the annulus when the pump is set at the formation and the dynamic liquid level is at the pump.

**FIGURE 6.7**

Pumping and shut-in conditions in the annulus when the pump is set at the formation and the dynamic liquid level is above the pump.

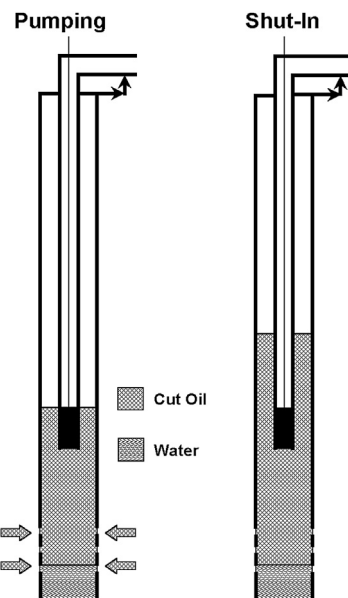


FIGURE 6.8

Pumping and shut-in conditions in the annulus when the pump is set above the formation and the dynamic liquid level is at the pump.

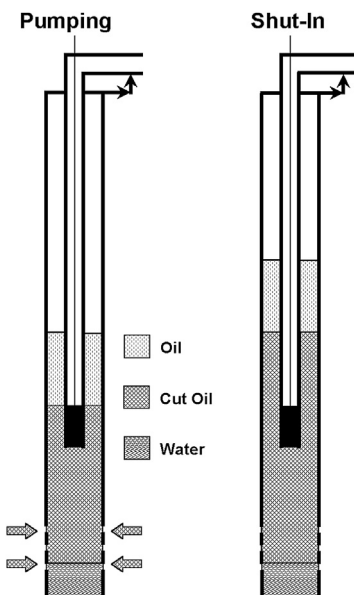


FIGURE 6.9

Pumping and shut-in conditions in the annulus when the pump is set above the formation and the dynamic liquid level is above the pump.

EXAMPLE 6.3: THE FOLLOWING CASE WILL BE USED IN SUBSEQUENT EXAMPLE PROBLEMS

Well depth is 6,000 ft with the pump set at the perforations. During pumping, the liquid level is at 5,500 ft, casinghead pressure is 100 psi. After shut-in, these parameters were measured as 4,500 ft and 450 psi, respectively. The well was previously tested and produced 300 bpd liquid with a WOR of 2. For simplicity, assume an average temperature of 80 F in the well, an oil gradient of 0.32 psi/ft, and a water gradient of 0.44 psi/ft. Specific gravity of the annulus gas is 0.75.

Calculate the static bottomhole pressure.

Solution

The gas column pressure, p_g , is calculated with a gas gradient of 14 psi/1,000 ft, read from Appendix A, corresponding to a surface pressure of 450 psi. Gas pressure is thus:

$$p_g = 4,500 \times 14/1,000 = 63 \text{ psi.}$$

To find the liquid column pressure, the composition of the static column must be determined. The 500 ft oil column present in the pumping case remains on the top of the static column. Liquid fill up from the formation equals the difference of pumping and static levels, i.e., $5,500 - 4,500 = 1,000$ ft. This additional column in the annulus contains the same amount of water as found in the previous production test. The static gradient of this column is found from the gradients of oil, water and the produced WOR:

$$1/3 \times 0.32 + 2/3 \times 0.44 = 0.4 \text{ psi/ft.}$$

Liquid column pressure is composed of the pressures due to 500 ft oil plus 1,000 ft water-cut oil columns:

$$p_l = 500 \times 0.32 + 1,000 \times 0.4 = 160 + 400 = 560 \text{ psi.}$$

Static bottomhole pressure is found from Eq. (6.18) as:

$$p_{ws} = 450 + 63 + 560 = 1,073 \text{ psi.}$$

6.2.3.3 Flowing conditions

In wells with negligible gas production, the calculation of flowing bottomhole pressures is quite simple and is accomplished with the method just described for static conditions. Usually, surface **casinghead pressure** is the main contributor to bottomhole pressure, but **liquid column pressure** can also be considerable. Again, it must be remembered that, under stabilized pumping conditions, all liquid above the pump is **oil** due to gravitational separation.

If formation **gas** is also produced, the calculation of bottomhole pressures is not so straightforward because, in these cases, the casing annulus contains a **gaseous liquid column**. It is customary to assume that most of the gas produced from the formation enters the **annulus**, and this gas continuously **bubbles** through the annular liquid column and leaves the well at the surface. The main effect of the produced gas is the **reduction** of the hydrostatic gradient of the annular liquid. In light of this, the accurate calculation of flowing bottomhole pressure (FBHP) heavily depends on the proper description of this phenomenon. In the following, the available correlations for liquid gradient correction are discussed first.

6.2.3.3.1 Annular pressure gradient

In a pumping well's annulus, a special case of multiphase **flow** takes place, since formation gas continuously bubbles through a **stagnant**, static liquid column. Depending on the gas volumetric rate, the flow patterns observed are **bubble flow** at low gas volumes and **slug flow** at higher gas rates. In both cases, the **density** of the mixture is found from the basic formula:

$$\rho_m = \rho_l H_l + \rho_g H_g \quad (6.19)$$

where:

- ρ_m = two-phase mixture density, lb/cu ft,
- ρ_l, ρ_g = liquid and gas densities, lb/cu ft,
- H_l = liquid holdup, –, and
- H_g = gas void fraction, –.

The contribution of gas density to **mixture** density is negligible and, therefore, can be deleted from the equation. Since hydrostatic pressure gradient is directly proportional to liquid density, the **gradient** of the gassy liquid column can be expressed with the gradient of the gas-free liquid as:

$$\text{grad}_m = \text{grad}_l H_l \quad (6.20)$$

where:

- grad_m = hydrostatic gradient of the gassy annular liquid, psi/ft,
- grad_l = hydrostatic gradient of the gas-free annular liquid, psi/ft, and
- H_l = liquid holdup, –.

The liquid holdup, H_l , can be considered as a **correction** of the liquid gradient; hence it is also called **gradient correction factor**. Due to its practical importance in flowing bottomhole pressure calculations, several correlations are available to determine its value. The earliest correlation, the **Gilbert S curve** [22], is shown in Fig. 6.10. Gradient correction factor (H_l) is plotted against the following group of parameters:

$$Q/A/p^{0.4}$$

where:

- Q = annular gas flow rate, Mscf/d,
- A = annular cross-sectional area, sq in, and
- p = actual column pressure, psi.

Godbey and Dimon [8] conducted a thorough investigation of the different possible flow patterns and gave two equations:

for **bubble** flow, $v_{sg} \leq 2$ ft/s:

$$H_l = 1 - \frac{v_{sg}}{1,2 v_{sg} + 0.183} \quad (6.21)$$

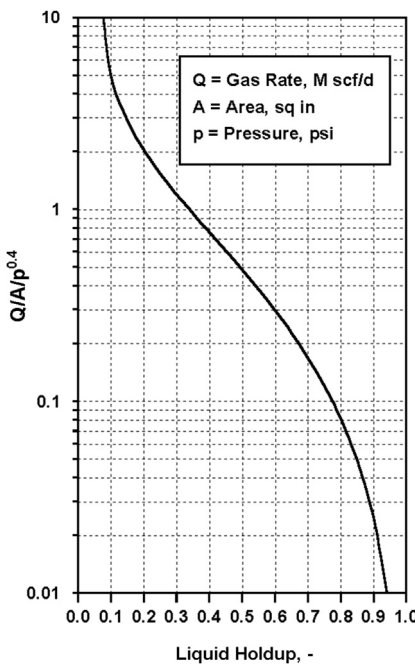
for **slug** flow, $v_{sg} > 2$ ft/s:

$$H_l = 1 - \frac{v_{sg}}{v_{sg} + 0.305} \quad (6.22)$$

where:

- H_l = liquid holdup (gradient correction factor), –, and
- v_{sg} = superficial velocity of the gas phase, ft/s.

With both methods, either the gradient correction factor can be calculated for the **average** conditions of the gassy liquid column or a step-wise procedure can be used to find different correction factors for different liquid levels.

**FIGURE 6.10**

Gilbert's gradient correction factor correlation, after [Gipson and Swaim \[22\]](#).

EXAMPLE 6.4: CALCULATE THE GRADIENT CORRECTION FACTOR FOR THE WELL DATA GIVEN IN [EXAMPLE 6.3](#), WITH BOTH THE GILBERT AND THE GODBEY-DIMON CORRELATIONS. ADDITIONAL DATA ARE: ANNULAR CROSS-SECTIONAL AREA OF 15 SQ IN, MEASURED ANNULAR GAS FLOW RATE OF 40 MSCF/D

Solution

No step-wise calculations are used for the **Gilbert** correlation; only a single correction factor is sought for the entire liquid column. For this purpose, a first guess of the average pressure is the pressure at the mid-height of the gas-free liquid column. Gas column pressure is assumed as 30 psi, and average pressure is the sum of surface, gas, and liquid column pressures:

$$p = 100 + 30 + 500/2 \times 0.32 = 130 + 80 = 210 \text{ psi.}$$

The correlating group of Gilbert is found as:

$$Q/A/p^{0.4} = 40/15/210^{0.4} = 0.31.$$

From [Fig. 6.10](#), the correction factor is read off as:

$$H_l = 0.58.$$

For the second iteration, the average pressure is adjusted by including the effect of annular gas in the liquid gradient, which is $0.32 \times H_l = 0.32 \times 0.58 = 0.185 \text{ psi/ft}$:

$$p = 100 + 30 + 500/2 \times 0.185 = 130 + 46 = 176 \text{ psi.}$$

The new value of the correlating group is:

$$Q/A/p^{0.4} = 40/15/176^{0.4} = 0.34.$$

The new correction factor from Fig. 6.10 is:

$H_l = 0.57$, which is close enough to the previous value and is the result of the calculations.

For the **Godbey-Dimon** correlation, the average liquid column pressure calculated previously is used. Additionally, gas deviation factor is assumed to equal $Z = 0.8$, for speeding up the calculation process. Gas superficial velocity, by definition, equals the actual gas volumetric rate divided by the cross-sectional area. The volume factor of the gas is found from:

$$B_g = 0.0283 \times Z \times T/p = 0.0283 \times 0.8(80 + 460)/176 = 0.07.$$

Superficial velocity of gas is:

$$v_{sg} = Q \times B_g / A = 40,000/86,400 \times 0.07/(15/144) = 0.31 \text{ ft/s.}$$

Since $v_{sg} < 2$ ft/s, bubble flow pattern exists and Eq. (6.21) is to be used:

$$H_l = 1 - 0.3/(1.2 \times 0.3 + 0.6) = 0.69.$$

Of the several **other** published correlations [23–25], the technique proposed by **McCoy et al.** [26] and used by the **Echometer** company should be discussed here. The gradient correction factor of these authors was based on field **measurements** and is reproduced in Fig. 6.11. Its use eliminates the often difficult determination of annular gas **flow** rates. For this purpose, the casing valve is closed in for a short period of time, while the pump is operating and the casing pressure **buildup** rate is recorded. For best results, a minimum pressure increase of 10 psi or a 10-min test period should be used. From these data, the following parameter group is calculated:

$$L' dp/dt$$

where:

dp = casing pressure buildup, psi,

dt = pressure buildup time, min, and

L' = corrected dynamic liquid level, ft.

The gradient **correction** factor (H_l) is then found from Fig. 6.11, where the definition of the corrected liquid level is:

$$L' = L + (1 - H_l)h_l \quad (6.23)$$

where:

L = measured depth of the dynamic liquid level, ft,

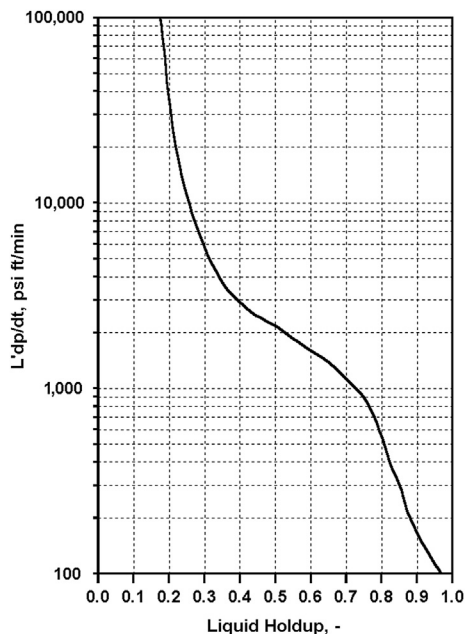
H_l = gradient correction factor, –, and

h_l = height of the gaseous liquid column, ft.

As seen above, calculation of the correction factor requires an **iterative** process, because H_l figures in the corrected dynamic liquid level that, in turn, is used to correlate H_l in Fig. 6.11. Usually, only a few iterations are necessary to converge to the proper value of the gradient correction factor, if a starting value of $H_l = 1$ is used.

FIGURE 6.11

The gradient correction factor correlation of echometer, after McCoy et al. [26].



EXAMPLE 6.5: CALCULATE THE GRADIENT CORRECTION FACTOR WITH THE ECHOMETER TECHNIQUE FOR THE WELL DATA GIVEN IN EXAMPLE 6.3, IF THE MEASURED PRESSURE BUILDUP AT THE CASING HEAD IS 7 PSI IN 10 MIN

Solution

Assume a starting correction factor of $H_l = 1$. The corrected liquid level is by Eq. (6.23):

$$L' = 5,500 + (1 - 1)500 = 5,500 \text{ ft.}$$

The correlating group is found as:

$$L' dp/dt = 5,500 \times 7/10 = 3,850$$

Correction factor is read off from Fig. 6.11 as:

$$H_l = 0.36.$$

Use the calculated H_l to find a new corrected liquid level:

$$L' = 5,500 + (1 - 0.36)500 = 5,500 + 320 = 5,820 \text{ ft.}$$

The correlating group is thus:

$$L' dp/dt = 5,820 \times 7/10 = 4,074$$

Reading off from Fig. 6.11:

$$H_l = 0.35.$$

One more iteration is needed with a new corrected liquid level:

$$L' = 5,500 + (1 - 0.35)500 = 5,500 + 325 = 5,825 \text{ ft.}$$

The new correlating group is:

$$L' dp/dt = 5,825 \times 7/10 = 4,078$$

The correction factor that belongs to this value is $H_l = 0.35$, which is the final converged value of the gradient correction factor. The correction factors calculated in the previous example are much higher than the value found with the Echometer model, also observed by McCoy et al. [26].

6.2.3.3.2 Flowing bottomhole pressure

After the pressure gradient of the gaseous liquid column present in a pumping well's annulus has been determined, the flowing bottomhole pressure is calculated analogously to the static pressure:

$$p_{wf} = p_c + p_g + p_l \quad (6.24)$$

where:

p_{wf} = FBHP, psi,

p_c = casinghead pressure during normal pumping, psi,

p_g = hydrostatic pressure of the annular gas column, psi, and

p_l = hydrostatic pressure of the annular gaseous liquid column, psi.

As before, surface casing pressure, p_c , is **measured** at the surface, and gas column pressure, p_g , is found from the measured liquid level **depth**, L , by calculating the increase of pressure with depth in the static gas column. The last term of the equation is evaluated with the use of the gradient correction factor:

$$p_l = h_l grad_l H_l \quad (6.25)$$

where:

h_l = the height above the formation of the gaseous liquid column in the annulus, ft,

$grad_l$ = hydrostatic pressure gradient of the gas-free annulus liquid, psi/ft, and

H_l = gradient correction factor, –.

EXAMPLE 6.6: FIND THE BOTTOMHOLE PRESSURES FOR THE DIFFERENT CORRELATIONS USED IN THE PREVIOUS EXAMPLES

Solution

The hydrostatic pressure of the gas column is 30 psi, as calculated in [Example 6.4](#). Liquid column pressure is found from [Eq. \(6.25\)](#), and using the different values of H_l we get:

$$p_l = 500 \times 0.32 \times 0.57 = 91 \text{ psi for the Gilbert,}$$

$$p_l = 500 \times 0.32 \times 0.69 = 110 \text{ psi for the Godbey - Dimon, and}$$

$$p_l = 500 \times 0.32 \times 0.35 = 56 \text{ psi for the Echometer correlations.}$$

Flowing bottomhole pressures are calculated by using [Eq. \(6.24\)](#):

$$p_{wf} = 100 + 30 + 91 = 221 \text{ psi for the Gilbert,}$$

$$p_{wf} = 100 + 30 + 110 = 240 \text{ psi for the Godbey - Dimon, and}$$

$$p_{wf} = 100 + 30 + 56 = 186 \text{ psi for the Echometer correlations.}$$

6.2.4 DETERMINATION OF WELL INFLOW PERFORMANCE

Knowledge of the static and flowing (producing) **bottomhole** pressures allows the calculation of the well's **inflow performance curve**. Two basic models can be used: a **constant** productivity index (PI) or **Vogel's IPR** curve. The productivity index, by definition, is found from:

$$PI = \frac{q}{(p_{ws} - p_{wf})} \quad (6.26)$$

where:

PI = productivity index, bpd/psi,

q = measured liquid production rate, bpd,

p_{ws} = static bottomhole pressure, psi, and

p_{wf} = flowing bottomhole pressure, psi.

The use of **Vogel's IPR concept** [27] results in the ratio of the actual to maximum possible liquid flow rate:

$$\frac{q}{q_{\max}} = 1 - 0.2 \frac{p_{wf}}{p_{ws}} - 0.8 \left(\frac{p_{wf}}{p_{ws}} \right)^2 \quad (6.27)$$

where the parameter not defined above is:

q_{\max} = theoretical maximum production rate, bpd.

After q_{\max} is determined from the above formula, the well's **IPR curve** can be constructed, and that was the purpose of well testing. Well test data can be used in the evaluation of the capabilities of the given well, as well as in investigating any changes in rod-pumping system design.

EXAMPLE 6.7: CALCULATE THE PARAMETERS OF THE INFLOW PERFORMANCE RELATIONSHIPS FOR THE CASES IN THE PREVIOUS EXAMPLE

Solution

Liquid production rate was measured as 300 bpd and p_{ws} was found as 1,073 psi in Example 6.3. Using the different p_{wf} values, the following PI values are found from Eq. (6.26):

$$PI = 300/(1,073 - 221) = 0.35 \text{ bpd/psi for the Gilbert,}$$

$$PI = 300/(1,073 - 230) = 0.36 \text{ bpd/psi for the Godbey - Dimon, and}$$

$$PI = 300/(1,073 - 186) = 0.34 \text{ bpd/psi for the Echometer correlations.}$$

If the Vogel IPR formula is used (Eq. 6.27) then the ratio of the actual to maximum flow rates is:

$$q/q_{\max} = 1 - 0.2(221/1,073) - 0.8(221/1,073)^2 = 1 - 0.041 - 0.034 = 0.925 \text{ for the Gilbert,}$$

$$q/q_{\max} = 1 - 0.2(230/1,073) - 0.8(230/1,073)^2 = 1 - 0.043 - 0.037 = 0.920 \text{ for the Godbey - Dimon,}$$

$$q/q_{\max} = 1 - 0.2(186/1,073) - 0.8(186/1,073)^2 = 1 - 0.035 - 0.024 = 0.941 \text{ for the Echometer correlations.}$$

A comparison of the well's **absolute open flow potential**, as calculated with the use of the different correlations, follows:

Correlation	Open Flow Potential	
Gilbert	From PI equation 376 bpd	From Vogel IPR 324 bpd
Godbey-Dimon	386 bpd	326 bpd
Echometer	365 bpd	319 bpd

EXAMPLE 6.8: PERFORM A WELL TEST ANALYSIS ON THE WELL PRESENTED IN EXAMPLE 6.3, USING THE ECHOMETER PROCEDURE

Solution

Exhibit 6.1 contains input data and calculation results for this case.

WELL TESTING OF A PUMPING WELL
USING ECHOMETER'S TESTING PROCEDURE

D A T A o f W E L L Ex. 6.8 tested on Nov.17, 1991

Perforations at :	6000.0 ft	Casing ID :	5.000 in
Pump Set at :	6000.0 ft	Tubing OD :	2.375 in
Wellhead Temp. :	80.0 F	Bottomhole Temp. :	100.0 F

F L U I D P R O P E R T I E S

Oil Sp.Gr. :	0.8	Gas Sp.Gr. :	0.750
Water Sp.Gr. :	1.0	H2S Content :	0%
		CO2 Content :	0%

L A S T P R O D U C T I O N T E S T

Liquid Rate :	300.0 bpd	Water Cut :	66%
---------------	-----------	-------------	-----

M E A S U R E D T E S T D A T A

	Pumping	Static
Measured Liquid Levels :	5500.0 ft	4500.0 ft
Casing Pressures :	100.0 psi	450.0 psi
dp (Pressure Buildup) :	7.00 psi	
dt (Buildup Time) :	10.00 min	

C A L C U L A T E D R E S U L T S

Calculated Annular Gas Rate : 37.5 M scf/d

	Pumping	Static
Oil Column Height, ft	500.0	500.0
Gradient, psi/ft	0.3418	0.3419
Holdup	0.363	
Liquid Column Height, ft	0.0	1000.0
Gradient, psi/ft	0.0000	0.3992
Holdup	0.363	
Gas Column Pressure, psi	117.2	531.6
Oil Column Pressure, psi	62.0	171.0
Liquid Column Pressure, psi	0.0	398.9
Bottomhole Pressure, psi	179.2	1101.4

Calculated Productivity Index : 0.325 bpd/psi

Data of Vogel IPR : $q/q_{max} = 94.6\%$ $q_{max} = 317.0$ bpd

EXHIBIT 6.1

Detailed well test results for the well given in [Example 6.8](#).

6.3 DYNAMOMETER SURVEYS

The most valuable tool for **analyzing** the performance of the pumping system is the **dynamometer**, which records the loads occurring in the rod string. These loads can be measured either at the surface with a polished rod dynamometer or at pump depth with a special downhole measuring device. In both cases, rod loads are recorded versus rod displacement or pumping time, during one or more complete pumping cycles. Since the variation of rod loads is a result of all the **forces** acting along the rod string and reflects the operation of the pump as well as the surface pumping unit, an evaluation of these loads reveals valuable information on downhole and surface conditions. Accordingly, the performance of the downhole and surface pumping equipment is usually analyzed by running a **dynamometer survey** (also called **well weighing**) on the given well.

The first “weight indicators” or **dynamometers** were used in the early 1920s. Since then, both the hardware and the evaluation methods have considerably improved. Thus the early and mostly **qualitative** interpretations, which relied heavily on the analyst’s **skill** and previous experience, have evolved into the sophisticated, highly reliable, and **exact** analysis methods of today. Interested readers are advised to consult the many fine books devoted entirely to the subject [28–30].

The **proper** use of dynamometer techniques and the correct **interpretation** of measurement data are of utmost importance for the production engineer when he or she tries to increase the **profitability** of sucker-rod pumping. It is the **evaluation** of dynamometer surveys that forms the basis for accomplishing the following basic tasks:

- Reduction of lifting **costs**,
- Detection and prevention of equipment **failures**,
- Improvement of the **selection** and **application** of pumping equipment, and
- Increase of well **production**.

In the following, first the **hardware** of dynamometry is discussed and the basic types of available dynamometers along with their operational principles are detailed. The use of dynamometers follows, where the different procedures are described that allow the determination of various operational parameters of pumping. Finally, a basic treatment of the **interpretation** of dynamometer diagrams is presented. Torque loading of the gearbox, as well as the power requirements of pumping based on measured dynamometer cards, were discussed in Chapter 4.

6.3.1 BASIC DYNAMOMETER TYPES

6.3.1.1 Polished rod dynamometers

Polished rod dynamometers, as the name implies, are instruments recording polished rod **loads** during the pumping cycle. The conventional types are the **mechanical** and the **hydraulic** dynamometer, which both produce a continuous plot of polished rod **load** versus polished rod **displacement**, the so-called **dynamometer diagram** or card. Modern dynamometers are **electronic** devices that record the loads and displacements at the polished rod as a function of **time** and enable the analyst to accurately analyze the downhole conditions of sucker-rod pumps.

6.3.1.1.1 Conventional dynamometers

The **mechanical dynamometer** employs a steel **ring** as its load measuring device, which, being placed between the carrier bar and the polished rod clamp, carries the full polished rod load. The ring’s

deflection is directly proportional to the load applied, which is **recorded** (after mechanical magnification) on **paper** attached to a rotating drum. Since the rotation of the drum is controlled by the polished rod's vertical movement, the resultant record is a **trace** of polished rod loads against displacement. The mechanical dynamometer is a rugged device, and the **Johnson-Fagg** version was extensively popular in the oil field. The major **disadvantage** of its use is the need to stop the pumping unit before the dynamometer is installed on the polished rod.

The **hydraulic dynamometer** (a well-known version is the **Leutert** dynamometer [31]) can be installed without the need to **stop** the pumping unit and, therefore, has a definite advantage over the mechanical one. Its operational principle is shown in the schematic drawing in Fig. 6.12. Before the first application on a well, a special **spacer** is installed on the polished rod between the carrier bar and the polished rod clamp. The dynamometer with its two load-sensing hydraulic **pistons** can easily be installed, even while the unit is pumping, between the shoulder of the spacer and the carrier bar. After the dynamometer is in place, hydraulic **pressure** is applied to the pistons by activating the hand pump connected to the system. The pistons lift the spacer off the carrier bar and the polished rod load hereafter is fully **supported** by the hydraulic pistons only. Thus, changes in polished rod **loads** entail changes in the hydraulic **pressure**, which are recorded by a stylus that magnifies the displacement of a spring-retarded piston. The record is made on **paper** attached to a drum **rotated** by a pull cord, one end of which is affixed to a stationary point. The rotational angle of the drum, therefore, is directly proportional to the polished rod's instantaneous **position**, and the record obtained is a plot of polished rod **load** versus polished rod **displacement**.

To accommodate different well conditions, different-size drums can be used for different stroke lengths. In addition, the retarding **spring** can be changed to alter the dynamometer's **load** range. These

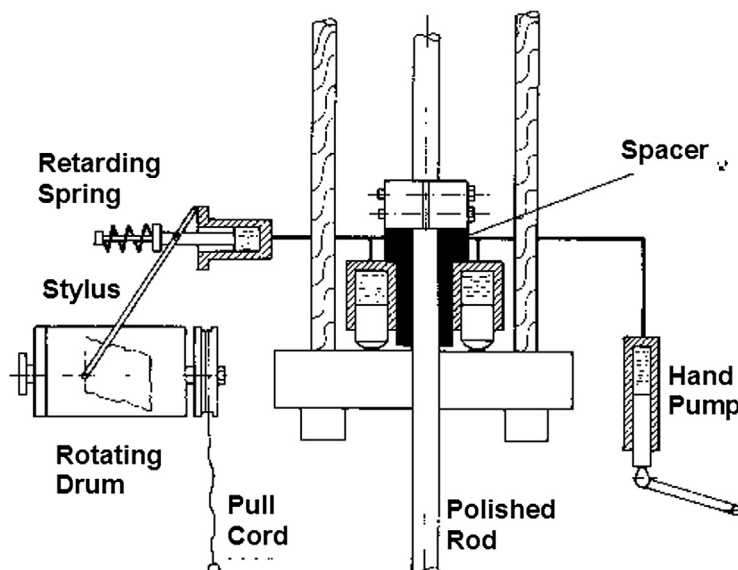


FIGURE 6.12

Schematic construction of a hydraulic dynamometer.

adjustments are easily carried out in the field, an added advantage of the use of such dynamometers. Thus, the recorded dynamometer diagram (or **card** for short) can be produced in a size that is easily interpreted.

The main **limitations** of the hydraulic (Leutert) dynamometer are the following [32]:

- Accuracy may deteriorate with the age of the instrument because the measuring spring weakens.
- They have a high amount of hysteresis caused by the drag (a) on the small piston that works against the retarding spring and (b) arising in the registration unit. Drift of measured loads can be expected.
- Load and position data are not available as a function of time, a basic requirement for the solution of the wave equation.

6.3.1.1.2 Electronic dynamometers

The **electronic** dynamometer's basic feature is that electronic **transducers**, rather than mechanical or hydraulic devices, are used for measuring well loads and rod displacements. As shown in Fig. 6.13, the main parts of such a dynamometer unit are the **load** transducer (load cell), the **position** transducer, and the **electronics**, which provides interfacing, signal recording, and processing.

The signals of both transducers, in forms of electric potential changes, are connected to data acquisition circuitry, which produces smoothed electric signals for recording and further processing. Polished rod load and position can thus be recorded on the optional portable **recorder** as a function of time. As seen earlier, this type of recording is a basic requirement when the solution of the damped **wave equation** is desired. Thus, a dynamometer of this type not only allows **surface** cards to be obtained but supplies the basic data for the construction of **downhole** cards as well.

The first electronic dynamometer was the **Delta II**, developed by **Shell Oil Co.** and widely used for obtaining data for downhole card calculations [33,34]. Later units included **microcomputers**

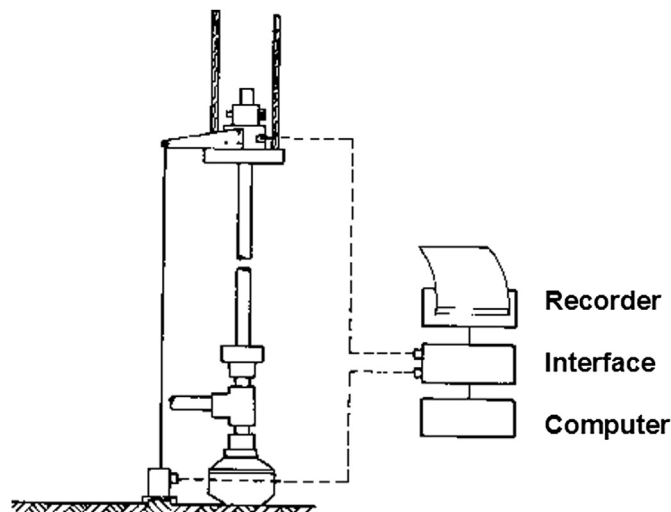


FIGURE 6.13

The main components of an electronic dynamometer.

and permitted the online analysis of measurements as well as easy data storage and retrieval operations. Today several companies offer **portable** electronic dynamometer systems controlled by **notebook** computers that perform real-time data acquisition functions and can also be used to calculate downhole cards [35–37].

Position Transducers

The earliest position transducers were spring-loaded **potentiometers** rotated by a string attached to the carrier bar; later on, **inclinometers** attached to the walking beam became popular. Both of these devices produce an **analog** signal directly proportional to polished rod displacement that is recorded as a function of time. Their common limitations are the insufficient resolution at the top and bottom of the polished rod stroke length, susceptibility to wear, and maintenance and calibration difficulties.

Accelerometers used in dynamometer systems eliminate the resolution and other problems; this is why they are becoming the preferred method to determine the variation of polished rod position. They are extremely small units permanently attached to the load sensing device. Such transducers accurately measure the polished rod's **instantaneous** acceleration, which, after being integrated twice with respect to time by the proper instrumentation, provides an accurate determination of the polished rod position versus time function [38]. The resolution of accelerometers is a function of the data sampling frequency and can thus be almost **continuous**; abrupt changes in polished rod velocity are easily recognizable.

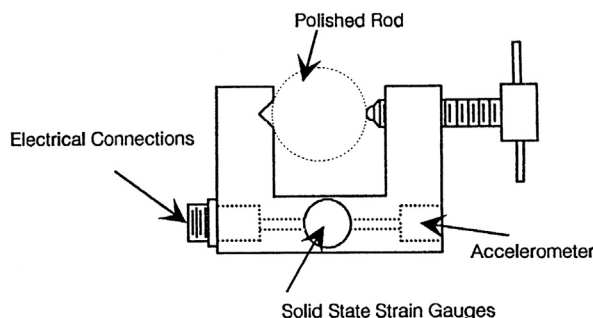
Load Transducers

There are several versions of load transducers (aka load cells) used in electronic dynamometers and for pump-off control [39]. The **horseshoe**-type load cell, if properly calibrated, indicates **actual** loads and is the most **accurate**, with an accuracy of 0.5% or better of its rated load. During measurement it is placed between the carrier bar and the polished rod clamp. It contains several (usually 12) **strain gauges** distributed cylindrically around the polished rod. The circular distribution of the strain gauges provides an averaging effect; side loading resulting from a tilted carrier bar does not affect measurement accuracy. Horseshoe transducers are quite expensive and are not used in pump-off control applications.

The **disadvantages** of using horseshoe load cells are that (1) the pumping unit must be **stopped** while placing the dynamometer on the polished rod, and (2) while mounting the cell on top of the carrier bar the rod string must be **raised** by about 3 inches, the height of the dynamometer. Since at the same time the downhole plunger (in respect to the pump barrel) is raised by an identical vertical distance, the **spacing** of the downhole pump will also change. This may bring about changes in pumping conditions and the dynamometer cards obtained will not represent normal pumping operations. Use of a properly dimensioned **spacer** on the polished rod can solve this problem.

Polished rod transducers (PRTs) measure the changes in **diameter** of the polished rod due to pumping loads using solid-state strain gauges [40,41]. As shown in Fig. 6.14, the transducer is lightly **clamped** to the polished rod below the carrier bar by tightening its screw; it contains the strain gauges measuring the loads as well as the **accelerometer** to determine polished rod positions. These transducers are very easy to mount on the polished rod and can provide a much **safer** application than horseshoe types.

The operational principle of PRTs is that **axial** loads on the polished rod create **radial** strain that is recorded by the unit and is converted to electric voltage signals. Output signal is **linear** as a function of load and the transducer has very little **hysteresis**; temperature effects are eliminated by a compensation circuit. The loads calculated from the output of the device are, however, **relative** in nature

**FIGURE 6.14**

The general arrangement of a polished rod transducer.

because the polished rod is already under tension when the load cell is installed. This requires the application of an **offset** to the raw data, which must be obtained during calibration.

Calibration is done using a **reference** load like the buoyant rod weight, or it is automatically performed by using the proper software. The software utilizes the solution of the wave equation and calculates the downhole dynamometer card; loads are then calibrated so as to have the **bottom** of the downhole card lie on the **zero** load line. After applying the same correction to the surface load data, the estimated surface dynamometer card is drawn.

The biggest **advantages** of PRTs are their **easy** application and the fact that the **spacing** of the downhole pump is not affected during the dynamometer survey because the polished rod need not be raised. An important benefit is that the sensitivity of the transducer does not significantly change throughout its life. The accuracy of PRTs as compared to the accurate readings of horseshoe load cells is quite high: maximum deviations are below 2%, a small price for the increased **ease** of use and the much higher **safety** of operation [42].

Permanently mounted load cells come in two versions: attached to the polished rod or to the walking beam. Polished rod load cells in cylindrical shape (donut shape) are placed between the carrier bar and the polished rod clamp; they utilize strain gauges, too. Measurement with such devices can be in error because they or their cabling are easily damaged and can drift out of calibration. Beam-mounted transducers are **welded** or **clamped** to the top of the walking beam near the center bearing and sense the flexing of the beam due to pumping loads. Their use eliminates the possibility of mechanical damage of signal cables, but measurement accuracy changes with ambient temperature because tension in the beam varies with the temperature of the beam. Permanently mounted load cells are most popular in conjunction with **pump-off** controllers (POCs) or as end devices in **supervisory control and data acquisition** systems.

6.3.1.2 Downhole dynagraphs

Dynamometer cards taken at the surface can seldom be used directly to detect the operating **conditions** of the downhole pump, because they also reflect all **forces** (static and dynamic) that occur from the pump up to the wellhead. If, however, a dynamometer is placed just **above** the pump, the recorded card is a true **indicator** of the pump's operation. This is what **Gilbert's dynagraph** (a mechanical dynamometer) [43] accomplished in the 1930s. Rod loads immediately above the

pump, recorded as a function of pump position, give **dynagraph cards**, a name used to distinguish them from surface cards. Although the application of **Gilbert's** dynagraph allowed a direct investigation of pumping problems, the practical **implications** associated with the necessity of running the instrument in the well had far outweighed its advantages. This seems to be true even for a modern, microprocessor-based version of the original instrument [44].

In order to provide the industry with high-quality measurements of sucker-rod pump dynamics, **Sandia** National Laboratories in 1997 conducted a series of measurements with **downhole** memory tools in sucker-rod-pumped wells [45]. The downhole sensors recorded pressure, temperature, load, and acceleration at several points along the rod string, including one immediately above the pump. A total of six wells were investigated under widely different operating conditions; their depths ranged from 2,600 to 9,300 ft. Sandia developed a downhole dynamometer **database** that includes all surface and downhole measurements and allows the construction of dynamometer cards at the different depths where sensors were installed [46]. Measured loads are "true loads" and pump cards obtained from the survey provide an efficient tool to compare the merits of different diagnostic and predictive computer program packages.

6.3.2 THE USE OF CONVENTIONAL DYNAMOMETERS

6.3.2.1 Recording a dynamometer card

Although this section is not intended as an operational guide for dynamometer measurements, some basic considerations for **conducting** a proper dynamometer survey will be discussed. By following the basic guidelines given below, dynamometer cards **representing** the current conditions can be taken, which, after being properly interpreted, provide a firm basis for an **analysis** of the pumping system [47]. It must be stressed, however, that the analysis of pumping wells does not consist of dynamometer measurements alone but includes other testing and measurement procedures as well. Therefore, to arrive at a final evaluation of the performance of the pumping system, all information gained from several analysis methods must be properly taken into account.

The basic rules to be followed **before running** a dynamometer survey when using a conventional dynamometer are:

1. Prior to dynamometer measurements, a fluid **level** survey must be run to ascertain the depth of the working fluid level present in the well.
2. Data of a current production **test** on the given well must be available, which give the latest oil, water, and gas production rates.
3. All relevant **data** on the given well and the pumping equipment must be collected and assembled. These include data on the equipment run in the well with types, sizes, depths, etc. Specific details of the tubing and rod strings, anchors, gas separators, etc. are a prime source of information. Equally important are surface equipment data: type, size of pumping unit, gear reducer, etc. Finally, the parameters of the current pumping mode (pump size, stroke length, pumping speed) must be recorded.

When **making** the dynamometer survey, the main points to remember are:

1. The **zero** load line should be recorded on the dynamometer card. This is accomplished by pulling the cord attached to the recording drum while no polished rod is applied.

2. The polished rod stuffing box should be **examined** for over-tightness and adjusted to keep friction on the polished rod at a minimum.
3. Before a representative card is recorded (the one taken under stabilized conditions), **several** cards on the same chart paper should be recorded.
4. After a correctly taken card is made, the subsurface pump's **valves** should be tested, and the actual **counterbalance effect (CBE)** must be recorded on the card. Both of these procedures are detailed in subsequent sections.
5. All relevant data (surface and subsurface) must be **recorded** on the card, along with the well's proper identification, to be used in later evaluations. A list of these parameters is **printed** on most types of dynamometer chart papers, which should be filled out by the analyst.

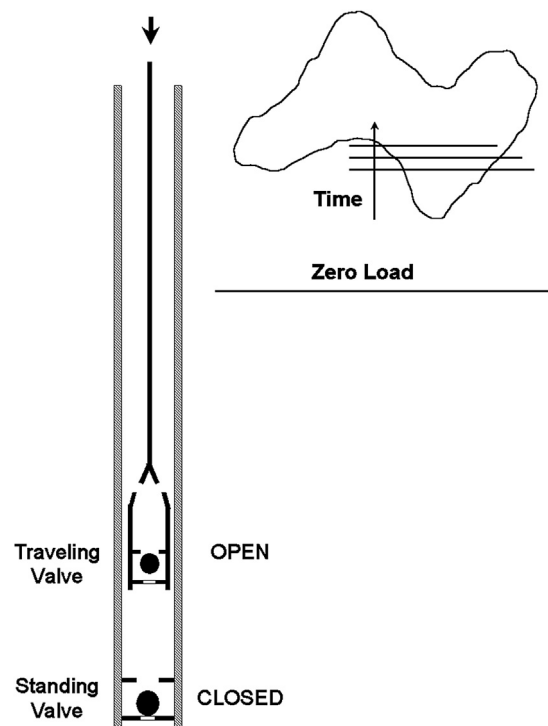
6.3.2.2 Checking the condition of pump valves

The proper operation of a sucker-rod pump is heavily affected by the **condition** of the standing and traveling **valves**. Both of these valves act as simple **check valves**, their operation depending on a proper **seal** between their seats and balls. However, due to mechanical damage, fluid erosion, corrosion, or other operational problems, valves can easily **lose** the perfect seal required for proper pump operation. Even the slightest **leak** can reduce the liquid rate lifted by the sucker-rod pump because of the high hydrostatic pressure valid at pump depth. The lifting capacity of the pump can thus considerably decrease with an associated deterioration of overall pumping efficiency. Therefore, it is of the utmost importance that the condition of the pump valves be **frequently** checked, which is fortunately quite easily accomplished with the use of a dynamometer.

6.3.2.2.1 The standing valve test

The standing valve test (**SV test**) is used to check the standing valve for **leaks** and is conducted with the dynamometer in place on the polished rod. At the start of the testing procedure, the pumping unit is **stopped** well into the **downstroke** (at about three-quarters of the way down) by switching off the motor and applying the brake. The unit must be stopped **gently** to eliminate any dynamic load effects. The actual polished rod load is immediately **recorded** on the dynamometer chart by pulling the cord of the dynamometer. As shown in Fig. 6.15, the standing valve is in a **closed** position, whereas the traveling valve is open. Since liquid load is completely carried by the **standing** valve, the polished rod load recorded at the commencement of the test represents the **buoyant weight of the rod string** only. In case the standing valve is in a **perfect** condition and holds well, the polished rod load remains **steady**. Thus, a repeated recording of the load by pulling the dynamometer cord again results in a line that falls on the first measurement. After **repeatedly** pulling on the cord at regular time intervals, no changes in polished rod load occur.

If the standing valve is **defective**, then it will leak fluids from the tubing due to the high pressure differential across its seat. As fluids leak from the space between the standing and traveling valves, the pressure immediately below the traveling valve will decrease, causing the traveling valve to **close** slowly. As time progresses, the traveling valve finally assumes the fluid load, which was originally carried by the standing valve. This **transfer of fluid load** will entail an **increase** in polished rod load, which is recorded at regular intervals (usually every second) on the dynamometer chart. As seen on the example card in Fig. 6.15, the original polished rod load (long horizontal line) **increases** as time progresses (indicated by the shorter lines), the rate of load increase being directly proportional to the **severity** of the standing valve leak.

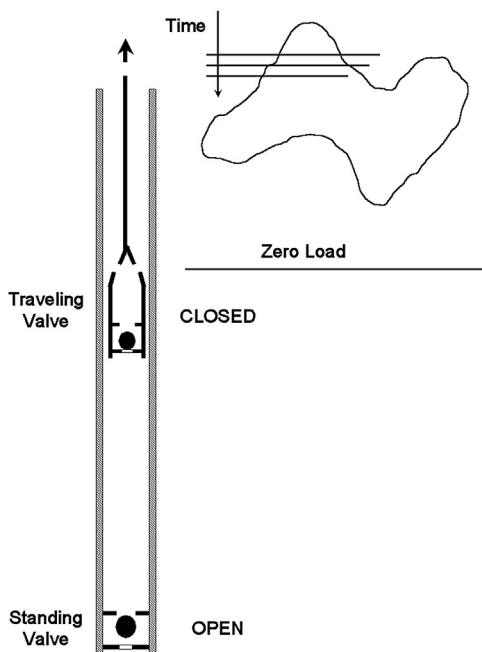
**FIGURE 6.15**

The principle of the standing valve test.

In case of leaking standing valves the valve test should be **repeated** several times to check for consistency. If the same results are obtained, then the **seat** of the standing valve is cut, whereas a damaged valve **ball** is indicated if the valve seems to hold on **some** trials. Usually, a leaking standing valve shows a load increase in about **20 s**. In no case should the measured load **decrease**; this indicates an **invalid** test, usually caused by stopping the unit before the traveling valve could open.

6.3.2.2.2 The traveling valve test

The traveling valve test (**TV test**) checks, with the same arrangement as used in the standing valve test, whether the traveling valve **and/or** the barrel-plunger fit is **leaking**. The pumping unit is **gently** stopped on the **upstroke** of the polished rod, near the top of the stroke. As the polished rod comes to a stop, the load on the dynamometer is immediately **recorded**. At this moment, the status of the pump valves is as shown in Fig. 6.16: the traveling valve is **closed** and the standing valve is **open**. The initial polished rod load, as recorded, represents the sum of the rod string weight in well fluids and the fluid load acting on the plunger. The standing valve is considered to be **open** and carries no load. If a perfect **seal** between the traveling valve seat and ball, and additionally, a perfect **fit** of the pump barrel and plunger, are assumed, then no **change** in polished rod load with time should

**FIGURE 6.16**

The principle of the traveling valve test.

occur. This condition is checked, as in the **SV test**, by pulling the cord of the dynamometer at several times in order to record the change in polished rod loads.

Any leakage in the traveling valve or between a worn pump barrel and plunger permits fluids to pass from **above** the traveling valve. This fluid leakage will slowly increase the pressure in the space between the pump's two valves, and the standing valve is **slowly** forced to close. As soon as it closes, the fluid load is no longer carried by the plunger and the rod string, but it is completely **transferred** to the standing valve and the tubing. The process of load **transfer** can be observed at the surface where polished rod loads are recorded on the dynamometer card at regular intervals. The original polished rod load, representing rod string weight plus fluid load, as recorded on the card (the long horizontal line on the example card in [Fig. 6.16](#)), is always **greater** than the loads measured **later** on. The rate of load decrease is, again, directly proportional to the leakage rates.

It should be clear from the above discussion that a **TV test** cannot differentiate between the effects of a leaking **traveling** valve and the leakage in the **pump** due to a worn barrel or plunger. As a rule, a measured loss in polished rod loads in about **5 s** is a positive indication of traveling valve leaks and/or an increased **slippage** past the plunger. As is the case with **SV tests**, the traveling valve test should also be **repeated** at different points in the upstroke. Differences in load loss rates observed during subsequent tests can indicate uneven wear or the position of a split in the pump barrel.

6.3.2.3 Measuring the counterbalance effect

With the use of a dynamometer it is possible to measure the **counterbalance effect**, i.e., the **force** at the polished rod arising from the **moment** of the counterweights. The proper knowledge of this parameter is a prime requirement for calculating the variation of **torques** on the speed reducer's slow-speed shaft. Two methods can be applied, depending on the actual degree of counterbalancing, which can show either an **over-** or **underbalanced** situation. If the pumping unit is overbalanced, or **weight heavy**, then, after stopping the motor and releasing the brake, the counterweights **lift** the polished rod. On the other hand, in a severely underbalanced or **rod-heavy** condition, the **polished rod** will **lift** the counterweights after the unit is stopped.

The counterbalance effect is measured with the dynamometer in place, carrying the full polished rod load. First the prime mover is shut down, and then the brake is applied slowly to **stop** the pumping unit with the **cranks horizontal** (this happens at crank angles of either 90° or 270°). At this position, the torque exerted on the crankshaft by the counterweights is at a **maximum**. This torque produces a vertical **force** on the polished rod, which is the *CBE* to be measured. In a **weight-heavy** situation, as shown in Fig. 6.17, the polished rod is **secured** by suitable means (a polished rod clamp and a chain) to the stuffing box, in order to prevent its vertical movement. Now the brake is completely **released**, and thus the mechanical moment of the counterweights is allowed to exert its effect on the polished rod. Since the polished rod is held stationary by the chain, the **force** that can be recorded with the dynamometer will give the actual *CBE* value. In **rod-heavy** cases, movement of the polished rod is prevented by installing a polished rod **clamp** directly over the stuffing box (Fig. 6.17). Again, after releasing the brake and pulling the cord of the dynamometer, the load recorded on the

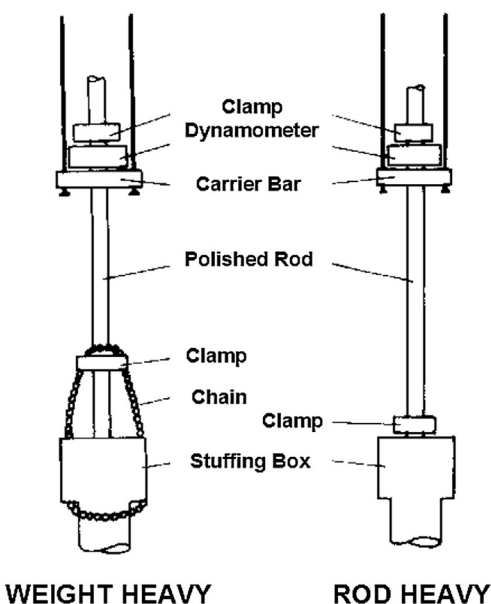


FIGURE 6.17

Two arrangements for measuring the counterbalance effect.

dynamometer card will correspond to the counterbalance effect. For greater accuracy measurements at both crank angles (90° and 270°) are made and the average of the two results is accepted.

From the *CBE* value measured above, the **maximum counterbalance torque** valid at the slow-speed shaft of the speed reducer is easily derived for any pumping unit geometry:

$$T_{CB\ max} = \frac{TF(90)(CBE - SU)}{\sin(90 + \tau)} \quad \text{if cranks stopped at } 90^\circ \quad (6.28)$$

$$T_{CB\ max} = \frac{TF(270)(CBE - SU)}{\sin(270 + \tau)} \quad \text{if cranks stopped at } 270^\circ \quad (6.29)$$

where:

$T_{CB\ max}$ = maximum counterbalance moment about the crankshaft, in lb,

$TF(\theta)$ = torque factor where *CBE* was measured (either 90° or 270°), in,

CBE = measured counterbalance effect, lb,

SU = structural unbalance, lb, and

τ = phase angle between the crank's and counterweight arm's centerline, degrees.

It is well known that the counterweights of pumping units other than conventional **geometry** are affixed to counterweight **arms** placed with an **offset** angle to the cranks. Hence, counterbalance torque is at a maximum when the counterweight **arms**, rather than the cranks, are in a **horizontal** position. In spite of this fact, the American Petroleum Institute (API) recommends [48] that *CBE* be determined with the **cranks held horizontal** during the measurement. Equations (6.28) and (6.29) account for this effect for nonconventional (**Torqmaster** and **Mark II**) pumping unit geometries.

EXAMPLE 6.9: FIND THE MAXIMUM COUNTERBALANCE MOMENT FOR AN M-228-213-86 UNIT, IF THE MEASURED VALUE OF THE *CBE* EQUALS 13,000 LB, AND THE UNIT'S STRUCTURAL UNBALANCE IS –2,040 LB. THE *CBE* WAS MEASURED AT A CRANK ANGLE OF 90° AND THE UNIT'S OFFSET ANGLE EQUALS 24.5°

Solution

The torque factor at a crank angle of 90° is found from Fig. 3.55 as 38 in.

The counterbalance moment is found from Eq. (6.28) as:

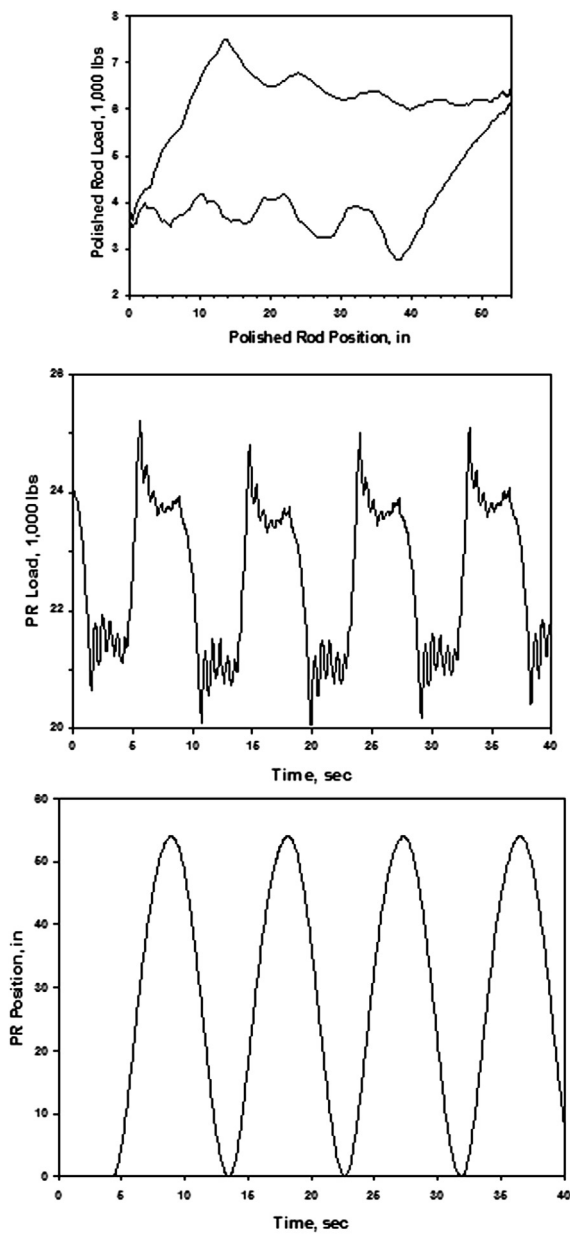
$$T_{CB\ max} = 38(13,000 + 2,040)/\sin(90 + 24.5) = 628,070 \text{ in lb.}$$

6.3.3 THE USE OF ELECTRONIC DYNAMOMETERS

6.3.3.1 Introduction

As detailed earlier, the modern electronic dynamometers record the polished rod load and displacement as a function of **time**. The **analog** signals of load and position transducers are converted to **digital** form by the proper electronic circuitry, then the digital signals are **sampled** at a fixed frequency. The usual sampling frequency is 50 ms, i.e., 20 samples per second; this ensures an almost continuous **resolution** and a very accurate description of the pumping system's operating conditions.

Load and position signals as received from the transducers are shown in Fig. 6.18 for an example case during several pumping cycles. Also plotted is the surface dynamometer card that can be constructed using these data for a given pumping cycle.

**FIGURE 6.18**

Typical load and position signals received from an electronic dynamometer.

The technique of running a dynamometer survey with the use of electronic dynamometers is very **similar** to that described in conjunction with the use of **conventional** dynamometers. Most of the **considerations** detailed earlier are still **valid** and the background theories of similar measurements are the same. This is the reason why the following sections should be read when a clear understanding of the principles and techniques detailed for conventional dynamometers has been achieved.

6.3.3.2 Recording a representative card

The main purpose of a dynamometer survey is to obtain a **representative** dynamometer card that properly characterizes the **stabilized** operation of the pumping system. Such cards represent the steady-state operation of the sucker-rod pump as well as other subsurface and surface equipment. It is quite easy to judge whether the pumping system's operation is stable when an electronic dynamometer is used by comparing the cards recorded during **consecutive** cycles. If the traces of several cards taken after each other fall closely on each other, then steady-state operation is reached and a representative card for further investigations can be acquired. Such a situation is illustrated in Fig. 6.19, where several cards closely overlap each other.

6.3.3.3 Checking the condition of pump valves

The most important components of the sucker-rod pump are the standing and traveling **valves**, and their actual mechanical condition greatly affects the operation of the pump. If they maintain a perfect **seal** between their seats and balls, then pump operation is basically **sound**; but the slightest **leak** can reduce the pump's liquid rate and the overall pumping efficiency. The mechanical condition of the valves of a sucker-rod pump is confirmed by running valve tests, i.e., the **standing valve test** and the **traveling valve test**.

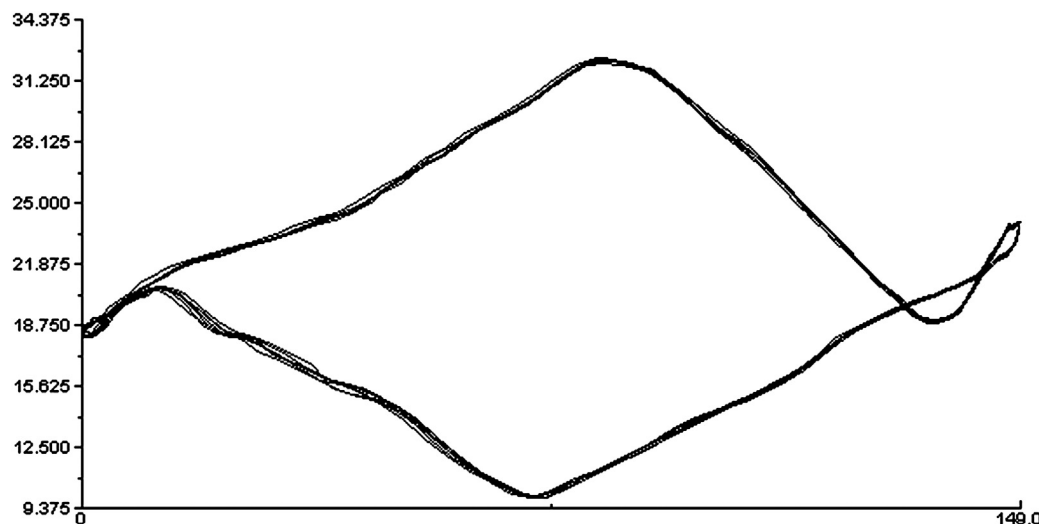


FIGURE 6.19

A sample steady-state, representative dynamometer card.

Standing Valve Test

This test is used to check the **condition** of the standing valve and it detects any **leaks** between the seat and the ball of the standing valve. The **SV test** is conducted with the electronic dynamometer installed on the polished rod while it continuously **records** the polished rod loads; test results are found from the **variation** of the recorded loads over a time period. It should be mentioned, however, that test results are valid only for negligible leakage in the pump, i.e., if the traveling valve and the plunger–barrel fit are in perfect condition.

At the start of the testing procedure the pumping unit is **stopped** on the **downstroke** when the polished rod is in the lower half of the downstroke by switching off the motor and applying the brake. In cases when there is an indication of a low pump fillage, the unit must be stopped very close to the bottom of the downstroke. When bringing the movement of the polished rod to a standstill, the application of the brake must be done **gently** and slowly to eliminate vibrations and dynamic load effects. As seen in Fig. 6.20, at the start of the **SV test** the traveling valve is in the **open** position, whereas the standing valve is in the **closed** position. The load recorded by the dynamometer at this time equals the rod string's **buoyant weight**, since the fluid load is completely carried by the standing valve. For a **perfectly** sealing standing valve this load does not change with time, as indicated on the dynamometer recording; measured loads will lie on a horizontal belonging to the **buoyant rod string weight**, seen at the position labeled **SV** in the figure. The measured rod string weight may be used to check the reliability of rod string data on file as well as to indicate the **accuracy** of the dynamometer's load cell by comparing it to the **calculated** buoyant weight.

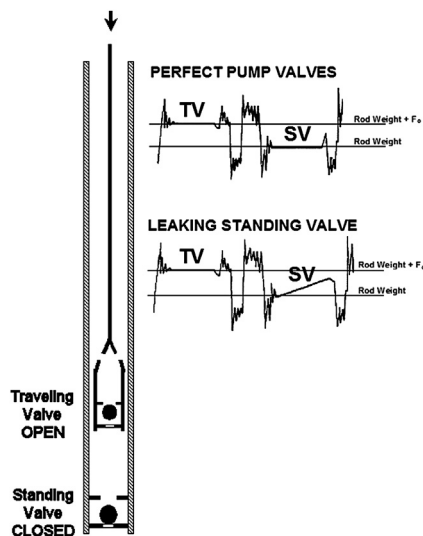


FIGURE 6.20

Typical standing valve test results from an electronic dynamometer.

A **leaking** standing valve, on the other hand, releases fluids from the tubing due to the high hydrostatic pressure differential across its seat, causing the pressure below the traveling valve to decrease. The traveling valve, being a simple check valve, starts to **close** because of the increasing

pressure differential from above; thus, the fluid load originally carried by the standing valve is gradually **transferred** to the traveling valve. As a result, the load recorded continuously by the dynamometer starts to **increase** from its original level (the buoyant rod string weight), as seen in Fig. 6.20 under the label **SV**. Any change in load indicates a leaking standing valve; the time rate of load increase is directly proportional to the **severity** of the standing valve leak. The **SV** test should be **repeated** several times to check for consistency.

Traveling Valve Test

This procedure detects **leaks** in the traveling valve **and/or** in the barrel-plunger fit due to pump wear; the **TV test** cannot differentiate between the effects of a leaking **traveling** valve and the leakage in the **pump** due to a worn barrel or plunger. The necessary arrangement is the same as used in the **SV test** and the test can be conducted before or after an **SV test**. At the beginning the pumping unit is stopped **smoothly** and slowly by switching off the motor and applying the brake; it must be stopped on the **upstroke** and near the top of the stroke. At this position, the downhole pump's valves are in the following state: the traveling valve is **closed** and the standing valve is **open**, as shown in Fig. 6.21. At this moment the dynamometer records a polished rod load equivalent to the sum of the **buoyant rod string weight** and the **fluid load** acting on the plunger, F_o , because the traveling valve carries all loads. In case the traveling valve operates **perfectly** and there is no leakage of fluids between the pump barrel and plunger, then the polished rod load must not change with time, at least not in a short period. This can be clearly detected on the electronic dynamometer's recording as a horizontal on the rod weight plus fluid load line under the label **TV**.

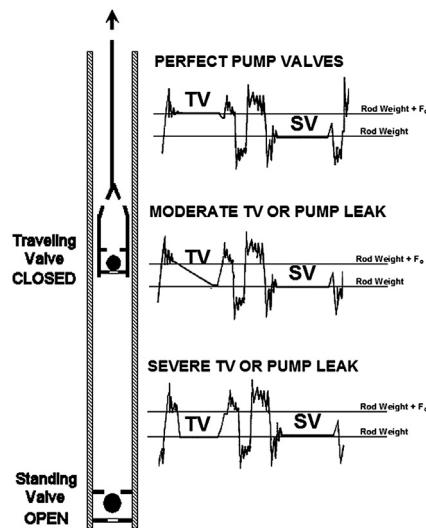


FIGURE 6.21

Typical traveling valve test results from an electronic dynamometer.

If there is a considerable **leakage** in the plunger-barrel fit of the sucker-rod pump and/or in the traveling valve itself, the fluid leaked increases the pressure above the standing valve. Because of this the standing valve begins to **close** and the **transfer** of the fluid load from the traveling to the standing

valve takes place. The polished rod load measured at the start of the TV test (sum of the buoyant rod string weight plus fluid load) will finally **drop** to the buoyant rod string weight. Since the decrease in polished rod load is continuously recorded by the dynamometer, observation of this change over time gives valuable information on the mechanical condition of the downhole pump. The rate of decrease in the measured load is, of course, directly proportional to the leakage rate. In case of a **moderate** leak, as shown in Fig. 6.21, it takes some time until polished rod load decreases to the level of the buoyant rod weight, as indicated by the recording under the label **TV**. A **severely** worn-out pump or a badly leaking traveling valve, on the other hand, is indicated by an **immediate** drop of load down to the level of the buoyant rod weight.

One has to consider that the effectiveness of leak detection by the **TV test** depends on the actual fillage of the downhole pump. With a fully charged barrel indicated by a **full** pump card, even a **slight** leak in the traveling valve and/or the plunger–barrel fit leads to a considerable drop in measured load, making the **TV test** a very **effective** leak detection method. On the other hand, in a pump with **low** fluid fillage more fluid must leak into the barrel before the fluid load is transferred to the standing valve, so leak detection is less effective. As a rule of thumb, a drop in polished rod load in about **5 s** is a positive indication of traveling valve **leaks** and/or an increased **slippage** past the plunger.

The **accuracy** of a **TV test** is related to stopping the pumping unit **smoothly** because the rod string may bounce back, which leads to erroneous readings. Also, the **TV test** gives reliable results only if the standing valve is holding perfectly during the test; otherwise, calculations would represent the valve that leaks at the greater rate. Similarly to the standing valve test, the traveling valve test should also be **repeated** by stopping the pumping unit at different points during the upstroke of the polished rod. Differences in load loss rates observed during subsequent tests can indicate uneven **wear** of the plunger or the barrel as well as the position of a **split** in the pump barrel.

6.3.3.3.1 Estimation of leakage rates

The change of the measured surface loads with time, as recorded during the TV and SV tests, allows the **estimation** of leakage rates in the pump. The following procedure, first proposed by **Nolen and Gibbs** [49], can be used to **infer** fluid leakage rates across the plunger–barrel fit and either the traveling valve or the standing valve; the calculation of the leakage in the pump will be detailed in the following [3].

As already discussed, during the **TV test** the fluid load is completely **transferred** from the rod string to the tubing if the plunger or the traveling valve leaks. As the load is removed from the plunger, the rod string loses its stretch caused by the fluid load and the plunger moves upward by a distance equal to that stretch. The volume of fluid that leaks past the pump needed to equalize the pressures above and below the plunger is the product of the net stretch and the pump's cross-sectional area. In case of an unanchored tubing string, the stretch of the tubing must also be taken into account and the leakage volume is derived as:

$$V = \frac{d^2\pi}{4} (e_r + e_t) \quad (6.30)$$

where:

V = leaked volume, cu in,

d = diameter of the downhole pump, in, and

e_r, e_t = elongations due to fluid load of the rod string and the tubing, respectively, in.

Leakage occurs only while the traveling valve is **closed** and when there is a pressure differential across it, i.e., at the start of the **TV test**. At that moment the load loss rate is at a **maximum**, $(\Delta F/\Delta t)_{\max}$, which can be determined from the plot of the measured load versus time curve obtained during the **TV test**. Considering that, at least for a full pump, the traveling valve carries the fluid load during the **upstroke** only, and converting the rate into bpd units, we get the final formula for pump leakage rate:

$$q_s = 3.5d^2 \left(\frac{\Delta F}{\Delta t} \right)_{\max} \left(\sum_{i=1}^{Taper} L_i E_{ri} + L_t E_t \right) \quad (6.31)$$

where:

q_s = pump leakage (slippage) rate, bpd,

d = diameter of the downhole pump, in,

$(\Delta F/\Delta t)_{\max}$ = maximum load loss rate, lb/s,

E_{ri} , E_t = elastic constant of the i^{th} rod taper and the tubing, respectively, in/(lb ft),

L_i , L_t = length of the i^{th} rod taper and the tubing, respectively, ft, and

Taper = number of rod tapers in string, –.

As pointed out by many investigators, the above procedure yields only an approximate value for the leakage in the pump.

6.3.3.4 Counterbalance effect measurement

The **counterbalance effect** is the **force** arising at the polished rod from the **moment** of the counterweights installed on the pumping unit; knowledge of this value is necessary for the calculation of the gearbox torque required to turn the counterweights. It can be easily measured with a dynamometer installed at the polished rod at the moment when the pumping system is at static equilibrium. At that moment the rod torque balances the counterbalance torque because inertial effects have vanished, and the counterbalance effect is found from the balance of the two torques.

The method frequently used with electronic dynamometers is based on the fact that polished rod loads will **inevitably** drop due to fluid **leakage** in the downhole pump after the pumping unit is stopped on the upstroke. Immediately after stopping the unit, the polished rod load equals the sum of the buoyant rod string weight and the fluid load ($W_{rf} + F_o$), but later on, due to fluid leakage in the pump, it drops down to the buoyant rod weight, W_{rf} . If the actual **CBE** lies somewhere **between** these two values, then at one moment it will **balance** the changing load on the polished rod; this time is found when no movement of the polished rod is detected. The main steps of the procedure are as follows:

1. The pumping unit is operated normally and the dynamometer is started to record polished rod position and load; a stopwatch is simultaneously started to measure elapsed time from this moment on.
2. The prime mover is shut down and then the brake is gently applied to **stop** the unit somewhere on the upstroke.
3. Now enough time is allowed for pump leakage to **reduce** the polished rod load and the brake is shortly **released** to check the movement of the polished rod.
4. If movement of the polished rod is detected, the brake is again applied to stop any movement. Since only **short** movements are allowed, these are much easier to detect on the brake **drum** than on the polished rod.

5. Periodic and momentary **release** of the brake is continued until no polished rod **movement** is detected with a completely released brake.
6. With the polished rod at rest, system equilibrium is reached and the load measured at the polished rod equals the *CBE*. The time when equilibrium occurs is noted on the stopwatch.
7. Using the polished rod position and load recordings of the dynamometer, the load *CBE* and position *s* valid at the time marked are determined.

The recorded polished rod position, *s*, allows the determination of the position of rods (*PR*) in the upstroke from:

$$PR = \frac{s}{S} \quad (6.32)$$

where:

PR = “position of rods” function, –,

s = recorded polished rod position at equilibrium, in, and

S = polished rod stroke length, in.

Using the kinematic parameters of the pumping unit (see Section 3.7.5), the crank angle, θ_e , and the torque factor, $TF(\theta_e)$, belonging to the *PR* value just calculated are determined. Using these parameters and the measured *CBE*, the **maximum counterbalance torque** at the slow-speed shaft of the speed reducer is easily derived similarly to Eq. (6.28):

$$T_{CB\ max} = \frac{TF(\theta_e)(CBE - SU)}{\sin(\theta_e + \tau)} \quad (6.33)$$

where:

$T_{CB\ max}$ = maximum counterbalance moment about the crankshaft, lb,

θ_e = crank angle where equilibrium occurs, degrees,

$TF(\theta_e)$ = torque factor at crank angle θ_e , in,

CBE = measured counterbalance effect, lb,

SU = structural unbalance, lb, and

τ = phase angle between the crank’s and counterweight arm’s centerline, degrees.

This procedure cannot be applied if the counterbalance effect is (1) greater than the sum of the buoyant rod weight and the fluid load ($W_{rf} + F_o$), or (2) less than the buoyant rod string weight, W_{rf} . These situations occur when the unit is very much **weight** or **rod** heavy. Another limitation is posed by fluid **slippage** in the downhole pump; installations with excessively high pump slippage cannot be analyzed because of the rapid drop in the loads measured by the dynamometer.

6.4 INTERPRETATION OF DYNAMOMETER CARDS

The correct **interpretation** of surface or downhole dynamometer cards reveals a wealth of **information** on the operation of the sucker-rod pumping system. The most **important uses** of dynamometer cards are the following:

- Determination of **loads** acting on the pumping unit structure and in the rod string.
- Based on dynamometer card data, the torsional **loading** on the pumping unit’s speed reducer can be calculated.

- From the area of the card, the **power** required to drive the pumping unit is found.
- By checking the actual counterbalance effect, the degree of the unit's counterbalancing can be determined.
- The condition of the sucker-rod pump and its valves can be determined.
- Many downhole **problems** can be detected by studying the **shape** of the dynamometer card, making the analysis of dynamometer cards a powerful **troubleshooting** tool.

6.4.1 CONVENTIONAL DYNAMOMETER CARDS

In order to understand the basic characteristic shapes of dynamometer cards taken at the surface with conventional dynamometers, cards for **simplified** conditions are discussed first. Assume a rigid, inelastic rod string; a sufficiently **low** pumping speed to eliminate dynamic forces; and pumping of an **incompressible** liquid; neglect all energy losses along the string; and assume an anchored tubing string. In this case the dynamometer card, i.e., the variation of polished rod load versus polished rod position, is represented by the parallelogram 1–2–3–4 shown in Fig. 6.22. At point 1, the upstroke begins and the traveling valve immediately closes. Polished rod load, equal to the buoyant weight of the string at point 1, suddenly **increases** to the load indicated by point 2, as the fluid load is **transferred** from the standing valve to the traveling valve. The plunger and the polished rod move **together** until point 3 is reached, while a constant load is maintained. In point 3, the end of the **upstroke** is reached, and the downstroke begins with the immediate **opening** of the traveling valve. Rod load suddenly **drops** to point 4, since fluid load is no longer carried by the traveling valve. The rod string, with the open traveling valve at its lower end, **falls** in well fluids from point 4 to 1, while polished rod load equals the buoyant weight of the rod string. At point 1, a new cycle begins.

Now, in a more realistic case, an **elastic** rod system is considered with all the other assumptions unchanged, and the shape of the dynamometer card changes to the **rhombooid** 1–2'–3–4' in Fig. 6.22. It is due to rod **stretch** that, from point 1, rod load only **gradually** reaches its maximum value at point 2', while the pump ascends with a **closed** traveling valve. Similarly, at the end of the

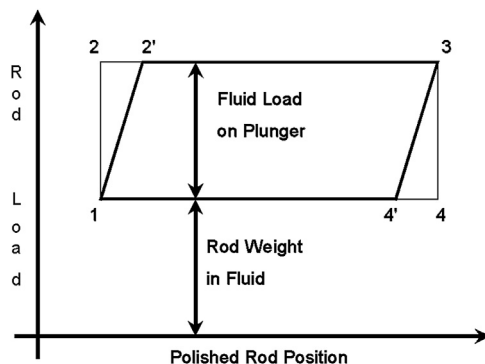


FIGURE 6.22

Theoretical surface dynamometer card shapes for low pumping speeds.

upstroke, the **transfer** of fluid load from the traveling valve to the standing valve is also **gradual** from point 3 to point 4', since the rod string contracts to its original length. This theoretical dynamometer card shape is seldom encountered and can only be found on shallow wells when slow pumping speeds are used [50].

It follows from the above description of the pumping cycle that, under the **simplified** conditions, maximum polished rod load equals the load measured during a traveling valve test, whereas minimum load equals that of the standing valve test. Another important conclusion, in line with the considerations detailed in [Section 6.3.2.2.2](#), is that plunger **travel** is less than the stroke **length** of the polished rod, the difference being taken up by rod string **elongation**. Hence, plunger stroke length 2–3, which is equal to polished rod stroke length for a rigid string, decreases to 2'–3 if the elasticity of the rod string is accounted for.

In a real well, the previous simplifying assumptions are **seldom** met because of the following:

- **Dynamic** rod loads occur due to the acceleration pattern of the rod string's movement;
- Stress **waves** are induced in the rod string by the polished rod's movement and by the operation of the downhole pump. These waves are **transmitted** and **reflected** in the rod string and can considerably affect the polished rod loads measured;
- The frequency of induced stress waves can **interfere** with the resonant (fundamental) frequency of the string, causing considerable changes in rod loads;
- The action of the pump valves is heavily affected by the **compressibility** of the fluids lifted; and finally;
- Downhole **problems** can exist that alter rod loads.

The **combined** effect of the above conditions changes the **shape** of the dynamometer card very significantly, as illustrated in [Fig. 6.23](#). As shown, maximum and minimum loads differ from the values valid for the slow-speed elastic rod model, and the general shape of the card is also distorted.

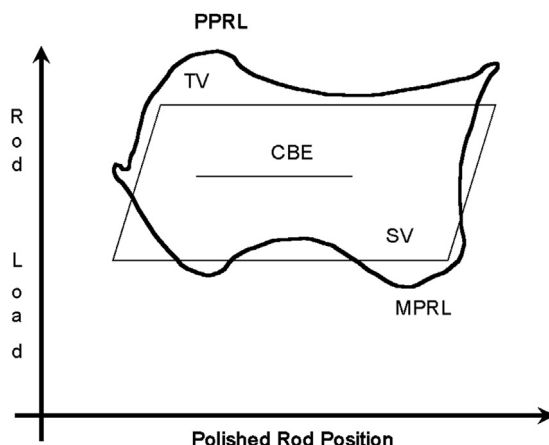
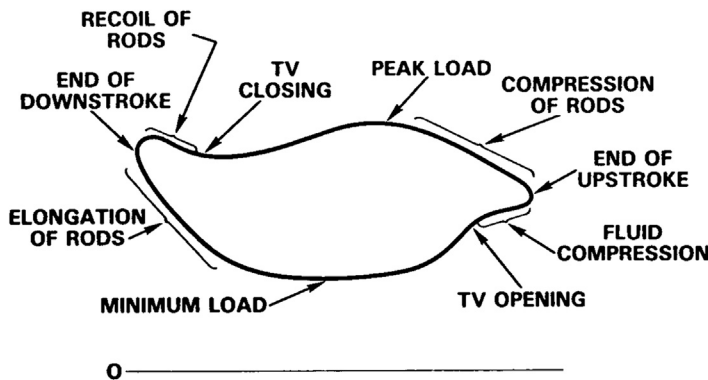


FIGURE 6.23

Comparison of an actual dynamometer card with a theoretical one valid at low pumping speeds.

**FIGURE 6.24**

Characteristic features of a general dynamometer card, after [Gipson and Swaim \[51\]](#).

Explanation of a **general** dynamometer card shape is given in [Fig. 6.24](#), after [Gipson and Swaim \[51\]](#). At the end of the polished rod's downstroke, the plunger still travels down due to the time delay in the string's stress transmission; hence the traveling valve (TV) closes only after the start of the polished rod's upstroke. After the traveling valve closes, the rods stretch and polished rod load increases until the peak load is reached. Toward the end of the upstroke, dynamic effects tend to compress the rod string, and polished rod loads decrease. The operation of the traveling valve is again delayed and it only opens after the polished rod starts its downstroke. The rods now start to contract and polished rod loads decrease to a minimum. Close to the end of the downstroke, dynamic effects dominate, causing the polished rod loads to increase again.

6.4.1.1 Basic loads

From a properly recorded dynamometer card, six basic **loads** can be determined, as pointed out by [Gipson and Swaim \[51\]](#). These are shown on the example card in [Fig. 6.23](#) and include:

1. The **zero load** or baseline from which all loads are measured.
2. The **SV load**, found from a standing valve test. In an ideal case, with the standing valve not leaking, the **SV load** equals the **buoyant weight** of the rod string.
3. The **TV load**, as measured during a traveling valve test. In cases where the plunger and the valves of the sucker-rod pump are in perfect condition, this load is the **sum** of the **buoyant rod weight** and the **fluid load** on the plunger.
4. The **peak polished rod load (PPRL)**, which is the maximum load during the pumping cycle and reflects the **TV load** plus the maximum of the dynamic loads occurring during the upstroke.
5. The **minimum polished rod load (MPRL)**, which represents the **SV load** minus the maximum downstroke dynamic load and is found on the dynamometer card as the minimum load during the cycle.
6. The **CBE**, which represents the force at the polished rod derived from the maximum counterweight moment.

The magnitude of the above loads is found from measuring the respective **ordinate** values above the zero load line on the conventional dynamometer **card**, and taking into account the spring constant of the dynamometer used.

6.4.1.2 Polished rod horsepower

Since the product of force and distance is mechanical **work**, the area enclosed by the dynamometer card represents the **work** done on the polished rod during a pumping cycle. From this, the **power** input at the polished rod is easily expressed with the pumping speed [52]:

$$PRHP = \frac{A_c K S N}{396,000 L_c} \quad (6.34)$$

where:

$PRHP$ = polished rod horsepower, HP,
 A_c = area of the dynamometer card, sq in,
 K = dynamometer constant, lb/in,
 S = polished rod stroke length, in,
 N = pumping speed, strokes/min, and
 L_c = length of the dynamometer card, in.

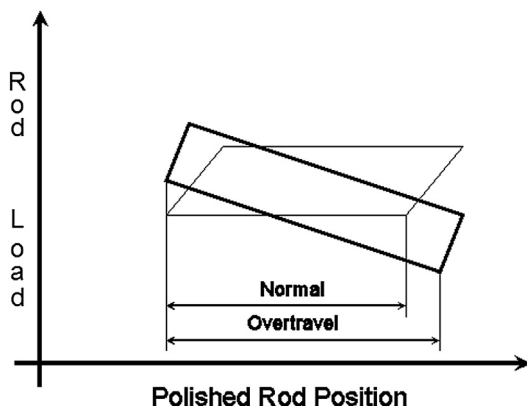
The polished rod **power** ($PRHP$) thus calculated is the **total** power required at the polished rod, which covers the **useful** power of fluid lifting and the sum of all energy **losses** occurring downhole. It is a very important parameter of sucker-rod pumping and clearly indicates the system's downhole **efficiency**, as already discussed in Section 4.7.

6.4.1.3 Troubleshooting

The detection of pumping **malfunctions** from the **visual** interpretation of surface dynamometer card shapes is a task for highly specialized analysts. Due to the many **interactions** of influencing parameters and the great number of possible pumping problems, an **infinite** number of dynamometer card **shapes** can exist, making the analysis of surface dynamometer cards more an **art** than an exact science. A proper troubleshooting analysis of the pumping system, therefore, heavily relies on the analyst's **expertise** and **skill**. A complete treatment of dynamometer card analysis, if it is possible at all, is beyond the scope of this section and only some basics are discussed in the following.

The shape of a **healthy** dynamometer card is mainly governed by the pumping **speed** and the **fluid load** on the plunger, though it is also influenced by additional parameters like the composition of the rod string, prime mover slip, etc. This fact was recognized by **Sucker Rod Pumping Research Inc.** when they developed an **analog** computer to **simulate** the operation of the pumping system. Their results, later adopted by the API in the **RP 11L**, made it possible to construct dynamometer cards for a multitude of **simulated** cases. These cards are published in **API Bul 11L2** [53], where dynamometer cards for good pumping conditions (100% fluid fillage of the pump, no gas interference, pump in perfect mechanical condition) are given. The cards are classified according to the values of two **dimensionless** parameters— N/N_o' and $F_o/S/k_r$ —because installations having identical such parameters have similar dynamometer cards shapes.

The use of **API Bul 11L2** in the analysis of dynamometer cards involves the calculation of the above dimensionless parameters, which are also used in the **RP 11L** procedure. Then, the analog card

**FIGURE 6.25**

The general shape of an overtravel card.

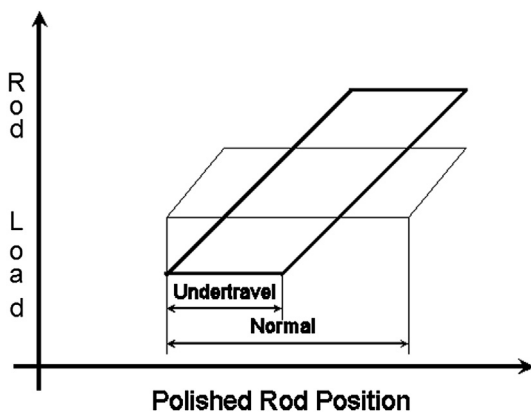
closest to these conditions is selected from the collection of cards found at the respective page of **API Bul 11L2**. If the measured card closely resembles the analog card just found, no apparent pumping problems are present; otherwise, further expert analysis is required.

According to their general shape, dynamometer cards are usually categorized as normal, overtravel, or undertravel cards. A typical **overtravel card** exhibits a general **downward** slope from left to right, like the theoretical card shown in Fig. 6.25. When compared to an ideal card shape, it is apparent that plunger stroke is **increased** for the same polished rod stroke length. This can be attributed to increased **dynamic** effects at higher pumping speeds when the increased acceleration of the heavy rod string results in greater stretch along the string. **Overtravel** has two effects on the operation of the pumping system: pump displacement increases (this is the main factor when fiberglass rod strings are used), but at the same time the frequency of rod and other failures also increases. Overtravel of the downhole pump normally occurs under the following conditions:

- higher-than-normal pumping speeds,
- when using a fiberglass rod string,
- if the rod string has parted downhole,
- if the pump unseats during the pumping cycle, and
- for gas-locked and worn-out pumps.

In **undertravel** situations (see Fig. 6.26), the card slopes **upward** from left to right and plunger stroke length is **decreased** when compared to polished rod stroke length. The reduced travel of the plunger is usually due to greater than normal downhole friction. Among the possible causes of undertravel are:

- **heavy** rod loads from the use of large plungers,
- excessive downhole friction because of sand or paraffin accumulation,
- a stuck pump,
- a too-tight stuffing box.

**FIGURE 6.26**

The general shape of an undertravel card.

6.4.2 CARDS FROM ELECTRONIC DYNAMOMETERS

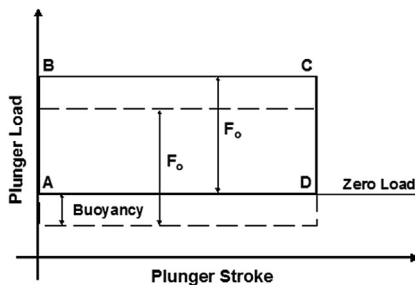
If an **electronic** dynamometer is used, then the dynamometer survey provides not only the **surface** card but also the calculated **downhole** card derived from surface dynamometer measurements by solving the **damped wave equation** that describes the behavior of the rod string. The use of downhole dynamometer cards offers a more **direct** detection of pumping **malfunctions** than the use of surface cards. This is mainly due to the fact that downhole cards, calculated at the depth of the sucker-rod pump, reflect the **operating** conditions of the pump alone. All other factors, e.g., rod string behavior and surface conditions, do not affect the loads and displacements occurring at this point. Pump cards usually have more **consistent** and more **characteristic** shapes than the surface cards they are derived from. Therefore, **pump cards** offer very efficient and reliable **indications** on the operational conditions of the sucker-rod pump and are widely used in troubleshooting the rod-pumping system [54–56].

Since pump cards are available immediately after the acquisition of surface dynamometer data, the use of electronic dynamometers offers a much higher level of **accuracy** and **reliability** than those provided by conventional dynamometers. This is the reason why today's sucker-rod pumping analysis relies heavily on the use of electronic dynamometers and the solution of the damped wave equation. The following sections discuss the basic concepts of dynamometer card analysis and the different ways of finding pumping parameters from dynamometer surveys.

6.4.2.1 *Ideal pump cards*

Before the interpretation of troublesome pump cards is attempted one must understand the features of cards obtained under **ideal** pumping conditions. The characteristics of ideal conditions for a sucker-rod pump can be summed up as follows:

- The pump's barrel and plunger are in **perfect** condition.
- The standing and the traveling valves are **not leaking**.

**FIGURE 6.27**

Ideal pump card for an installation with an anchored tubing string.

- All friction forces along the rod string are due to **viscous** damping.
- Only single-phase **liquid** enters the pump barrel.
- The barrel fills up **completely** during the upstroke.

Under such conditions pump cards calculated from the solution of the wave equation exhibit very characteristic and simple shapes, from which the most important pumping parameters are easily found. An ideal pump card for an installation with an **anchored** tubing string is given in Fig. 6.27. The loads plotted can be either **true** or **effective** rod loads, depending on the analyst's preference. Most investigators use effective loads and the card (the parallelogram A–B–C–D) sits on the zero load line; if true loads are considered then the card (indicated inside dashed line) is shifted downward by the **buoyancy** force acting on the bottom rod taper.

Investigation of the plunger's **movement** (position, velocity) during the pumping cycle can provide useful information on the behavior of the downhole pump. Figure 6.28 presents the variation of the polished rod's and the plunger's position for a complete pumping cycle for an ideal case with an **anchored** tubing string. The polished rod position is a very regular function of the elapsed time, as found from the **kinematic** analysis of the pumping unit's movement (see Section 3.2.5). The plunger with the closed traveling valve, on the other hand, does not start to move at the beginning of the upstroke (point A), while the load on the rods increases and the rod string gradually stretches. As soon as the load on the rods assumes the fluid load on the plunger (at point B) the plunger starts to move upward; the standing valve opens at the same time. The elapsed time for point B is found where the polished rod's position equals the stretch of the rod string due to fluid load:

$$e_r = \frac{F_o}{k_r} \quad (6.35)$$

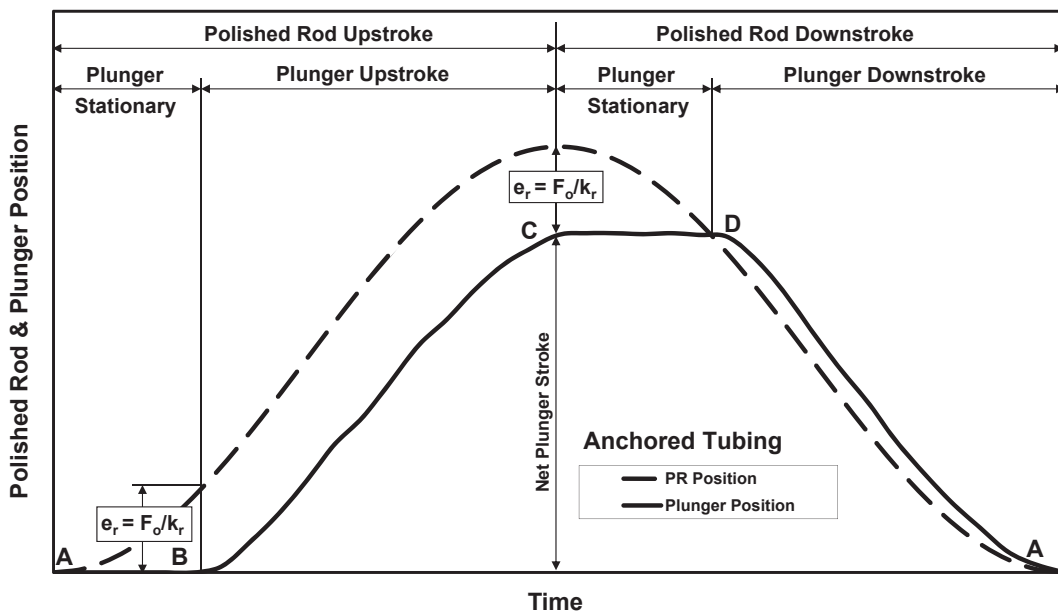
where:

e_r = stretch of the rod string due to fluid load, in,

F_o = fluid load on plunger, lb, and

k_r = spring constant of the rod string, lb/in.

The upstroke portion of the plunger's movement lies between points **B** and **C** where the plunger's position follows that of the polished rod. Downstroke starts at point **C**; the position of the plunger at this point defines the plunger's **net** stroke length. This stroke length is less than that of

**FIGURE 6.28**

Comparison of the polished rod's and the plunger's movement for an anchored tubing string.

the polished rod; the **difference** is the stretch of the rod string, e_r , defined previously. At the start of the downstroke the plunger stays **stationary** again while the rod string unstretches and the fluid load from the plunger is slowly transferred to the standing valve between points **C** and **D**. At point **D** the standing valve **closes** and the rod string is completely unloaded; the plunger falls until the end of the stroke is reached at point **A** again.

It can be concluded from the previous description of the plunger's movement that under ideal conditions, i.e., (1) nonleaking standing and traveling valves, (2) anchored tubing string, and (3) perfect fit between the plunger and the barrel, the plunger must not move between points **A–B** and **C–D**. Any change in plunger position or velocity in those ranges may indicate that some of the conditions are not met: valves may leak; tubing anchor may slip, etc.

The shape of the ideal pump card changes when the tubing string is **not anchored**, as shown in Fig. 6.29. From the start of the upstroke at point **A** the tubing string unstretches because the fluid load is transferred from the standing to the traveling valve. This is why the plunger moves upward by a distance equivalent to the stretch of the tubing before it carries the fluid load F_o at point **B**. Tubing stretch is found from the following formula:

$$e_t = \frac{F_o}{k_t} \quad (6.36)$$

where:

e_t = stretch of the tubing string due to fluid load, in,

F_o = fluid load on plunger, lb, and

k_t = spring constant of the tubing string, lb/in.

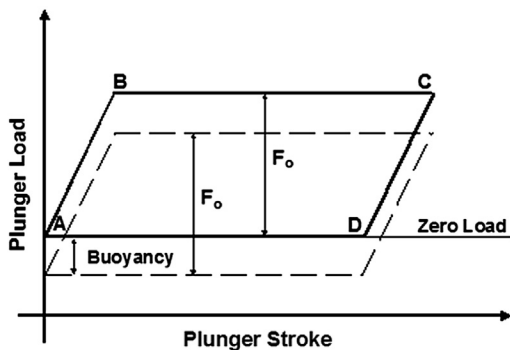


FIGURE 6.29

Ideal pump card for an installation with an unanchored tubing string.

At the end of the upstroke at point C the fluid load is transferred to the standing valve when the tubing stretches the amount given in Eq. (6.36); the plunger must move downward by the same distance as shown between points C and D.

The comparison of polished rod and plunger positions is presented in Fig. 6.30. At the start of the upstroke both the tubing and the plunger are moving between points A and B but in **opposite** directions. The tubing string gradually shortens because the fluid load on it is transferred to the

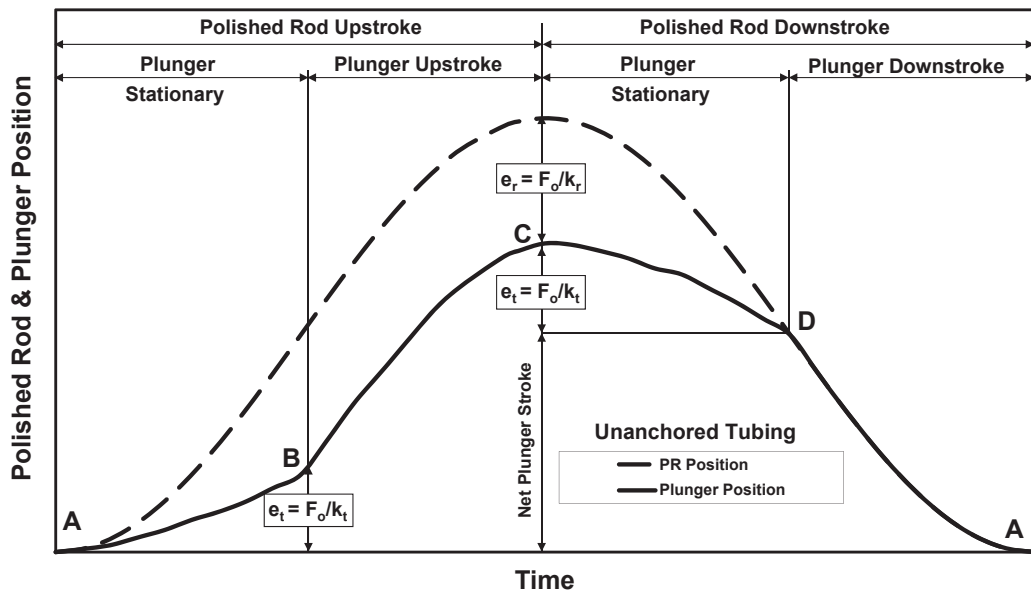


FIGURE 6.30

Comparison of the polished rod's and the plunger's movement for an unanchored tubing string.

plunger; the rod string, at the same time, is elongated. Due to the interaction of these movements the plunger stays **stationary** with respect to the pump barrel. When the plunger starts its upstroke at point **B**, it has covered a distance equal to the stretch of the tubing string, e_t . The plunger's movement attains its maximum at point **C**; plunger position here is less than the polished rod stroke length by the stretch of the rod string, e_r , found from Eq. (6.35).

Between points **C** and **D** the plunger does not move in relation to the barrel because its downward movement is eliminated by the tubing string's stretch, e_t , as the fluid load is transferred from the rod string to the tubing string. The **net** plunger stroke length is reached at point **D** and it is less than the maximum movement of the plunger (point **C**) by the stretch of the tubing string, e_t , found from Eq. (6.36). From point **D** on, the fluid load on the plunger is zero because the fluid load was transferred to the standing valve; the rod string is fully unstretched and moves the plunger during the rest of the downstroke in sync with the polished rod.

The investigation of plunger position versus time, as shown previously for ideal conditions, assists the analyst to evaluate and troubleshoot downhole problems. In addition to position data, evaluation of plunger **velocities** during the pumping cycle can facilitate the detection of pump problems. These methods of analysis are usually available in commercial wave equation program packages [57].

6.4.2.2 Basic analysis

When analyzing surface and downhole cards obtained from an electronic dynamometer survey, plotting of several **reference lines** on the cards greatly facilitates the analysis of the pumping system's operating conditions [58,59]. In the following we introduce these basic references and discuss how their use can improve the explanation of the pumping system's behavior.

6.4.2.2.1 Surface cards

The definitions of the basic reference lines to be used on the surface card are given in the following.

Buoyant weight of the rod string, W_{rf} : This represents the rod string's calculated weight in the produced liquid.

$$\begin{aligned} W_{rf} &= W_r(1 - 0.128 \text{ } SpGr) \\ &= (1 - 0.128 \text{ } SpGr) \sum_{i=1}^{\text{Taper}} L_i w_{ri} \end{aligned} \quad (6.37)$$

where:

W_{rf} = buoyant rod string weight, lb,

W_r = rod string weight in air, lb,

$SpGr$ = specific gravity of the fluid pumped, –,

L_i = length of the i^{th} rod taper, ft,

w_{ri} = weight of the i^{th} rod taper, lb/ft, and

Taper = number of rod tapers in string, –.

Maximum upstroke load, $W_{rf} + F_{o \text{ max}}$: This load represents the estimated maximum polished rod load when **pump-off** conditions are assumed. The theoretical **maximum fluid load** $F_{o \text{ max}}$ is

calculated by using the dynamic liquid level at the pump setting depth, i.e., by assuming a pump intake pressure of zero when the following formula is valid:

$$F_{o \max} = A_p (WHP + 0.433 L_{\text{pump}} SpGr) \quad (6.38)$$

where:

$F_{o \max}$ = fluid load on plunger during pump-off, lb,

A_p = cross-sectional area of the plunger, sq in,

WHP = wellhead (tubing head) pressure, psi, and

L_{pump} = pump setting depth, ft.

Spring constants calculated for unanchored and anchored tubing strings: These parameters indicate the probable **slope** of the surface dynamometer card at the start of the upstroke.

$$k_{r+t} = \frac{1}{\sum_{i=1}^{Taper} L_i E_{ri} + L_t E_t} \quad \text{for unanchored tubing} \quad (6.39)$$

$$k_t = \frac{1}{\sum_{i=1}^{Taper} L_i E_{ri}} \quad \text{for anchored tubing} \quad (6.40)$$

where:

k_{r+t}, k_t = spring constant of the rod + tubing and the tubing string, respectively, lb/in,

E_{ri}, E_t = elastic constant of the i^{th} rod taper and the tubing, respectively, in/(lb ft),

L_i = length of the i^{th} rod taper, ft,

L_t = length of the tubing string, ft, and

$Taper$ = number of rod tapers in string, –.

TV load: The measured load during the **TV test**.

SV load: The measured load during the **SV test**.

The use of the reference loads just discussed is illustrated in Fig. 6.31 where an example surface card is presented. The spring constant of the system gives an approximation of the slope of the card at

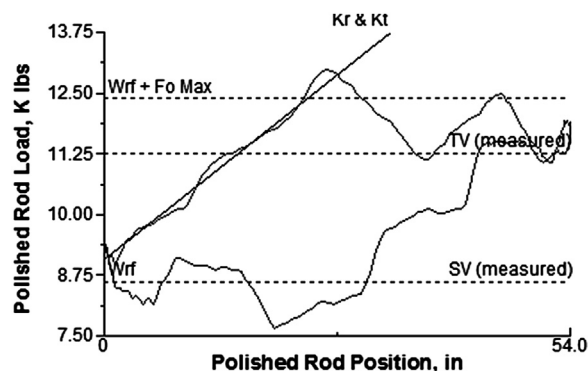


FIGURE 6.31

Reference load lines on a surface dynamometer card.

the start of the upstroke. In the given case a composite spring constant, $k_r + t$, representing the **concurrent** stretch of the tubing and the rod string, is depicted because the well's tubing string is not anchored. The results of the pump's valve tests can be used to estimate the actual fluid load on the plunger by subtracting the *SV load* from the *TV load*. These two loads can be used to detect any **unaccounted** friction loads in the pumping system; such loads cannot be described by the conventional wave equation, which assumes viscous damping only. The indications for high unaccounted friction are that *SV load* is less than the buoyant weight of the rod string, i.e., $SV \text{ load} < W_{rf}$, while *TV load* is greater than $W_{rf} + F_{o \text{ max}}$.

6.4.2.2 Pump cards

Downhole pump cards are calculated at the pump setting depth using the solution of the damped **wave equation**. Most software packages plot the pump card using **effective loads** in order to facilitate the detection of **buckling** conditions in the rod string. If effective loads are used, as discussed in Section 3.5.3.2.1, the pump does not carry any load during the downstroke and the pump card sits on the zero load line. The reference lines on calculated downhole cards are defined as follows.

Zero load line: If energy losses along the rod string are **entirely** due to viscous damping the downstroke loads should lie on the zero load line.

Maximum fluid load, $F_{o \text{ max}}$: As before, this theoretical load on the plunger is found by assuming **pumped-off** conditions and using Eq. (6.38).

Spring constant of the tubing string, k_t (calculated for cases of **unanchored** tubing): A line with the corresponding slope represents the **stretch** of the unanchored tubing string

$$k_t = \frac{1}{E_t L_t} \quad (6.41)$$

where:

k_t = spring constant of the tubing string, lb/in,

E_t = elastic constant of the tubing, in/(lb ft), and

L_t = length of the tubing string, ft.

Fluid load from fluid level, $F_{o \text{ FL}}$: This load is calculated from the differential pressure acting on the plunger on the **upstroke** and includes the effect of the pump intake pressure (*PIP*), which can be found from the measured dynamic liquid level in the annulus. *PIP* calculations involve running of an acoustic survey and the determination of annual liquid gradients as discussed in Section 6.2.3.3.2. Based on those parameters the fluid load on the plunger is calculated as follows:

$$F_{o \text{ FL}} = A_p (WHP + 0.433 L_{\text{pump}} SpGr_t - PIP) \quad (6.42)$$

where:

$F_{o \text{ FL}}$ = fluid load on the plunger, as calculated from the fluid level, lb,

A_p = cross-sectional area of the plunger, sq in,

WHP = wellhead (tubing head) pressure, psi,

$SpGr$ = specific gravity of the liquid in tubing, –,

L_{pump} = pump setting depth, ft, and

PIP = pump intake pressure, psi.

Fluid load from valve tests, $F_o \text{ VT}$: An approximation of the plunger's fluid load is obtained from the loads measured during a **valve test** procedure, as given here:

$$F_o \text{ VT} = TV \text{ Load} - SV \text{ Load} \quad (6.43)$$

where:

$F_o \text{ VT}$ = fluid load on the plunger, as calculated from valve tests, lb.

$TV \text{ Load}$, $SV \text{ Load}$ = loads measured during the TV and SV tests, respectively.

Estimated loads, F_{UP} , F_{DWN} : These loads and the corresponding reference lines are **estimated** by the analyst and their correct placement requires some experience. As discussed in Section 4.4, if the correct damping factor is used in wells with **negligible** unaccounted friction, the top and bottom sides of the pump card must be near **horizontal**. Since there is almost always some amount of unaccounted friction in the downhole environment, the cards always exhibit **uneven** top and bottom sides and the proper placement of the F_{UP} and F_{DWN} loads is intended to **separate** those frictional loads from the actual loads on the plunger. It is usually assumed that friction is about **equal** on the up- and the downstroke; therefore about the same loads are removed from the top and the bottom sides of the pump card by the two reference lines.

Gross plunger stroke: The gross plunger stroke length is found as the difference of the two **extreme** positions of the plunger's travel during the pumping cycle.

Net plunger stroke: This is the part of the plunger stroke length during which the plunger moves through fluid in the barrel on the downstroke.

The utilization of the reference lines just described is illustrated in Fig. 6.32, which depicts the downhole card calculated from the surface dynamometer card previously discussed along with the proper reference lines. The card is typical for an **unanchored** tubing string and the stretch of the tubing is properly described by the slope equal to the spring constant k_t of the tubing string. The loads on the downstroke being near zero clearly indicate that there are insignificant **unaccounted** friction loads present in the well.

The actual **fluid load** on the plunger can be estimated by different ways and the following results are obtained. An acoustic survey of the dynamic liquid level in the annulus allowed the

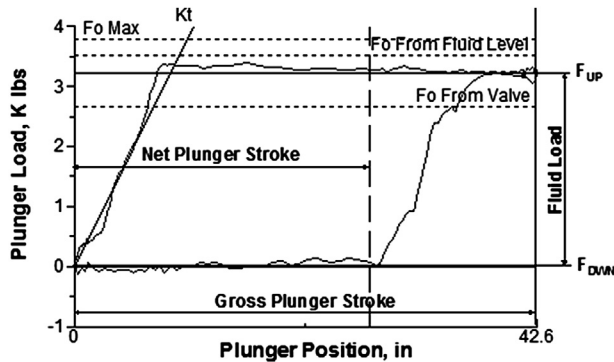


FIGURE 6.32

Reference load lines on a downhole pump card.

calculation of F_o FL = 3,508 lb; the valve tests resulted in F_o VT = 2,656 lb; whereas the placement of the F_{UP} and F_{DWN} lines gave a load of 3,285 lb, which is the accepted value. A comparison of the estimated fluid load to the theoretical maximum fluid load F_o max shows that the pump supplies most of the energy needed to produce the fluids i.e., the fluid level in the annulus is near the pump and the well's producing bottomhole pressure is low. Finally, the plunger's gross stroke length is read from the card as 42.6 in; net plunger stroke is estimated as 33.2 in; the difference is due to the fact that the barrel does not completely fill during the upstroke.

6.4.2.3 Detection of common pump problems

This section discusses the ways common pump problems may be detected from calculated pump cards. Such problems include incomplete pump fillage as well as a variety of mechanical troubles affecting the pump and/or its valves.

6.4.2.3.1 Incomplete pump fillage

Under **ideal** conditions the barrel of the downhole pump **completely** fills up with **incompressible** liquid during the upstroke of the pumping cycle and the full stroke length of the plunger is utilized to produce well fluids. Pump displacement, therefore, is found from the **gross** plunger stroke length, the pump size, and the pumping speed; in this case pump **fillage**, the ratio of the net and the gross plunger stroke lengths, is 100%. Liquid fillage rates below 100% are normally experienced in the field and this condition is basically caused by not meeting one or both of the basic **assumptions** for a perfect pump operation: the barrel does not fill up **completely**, and/or the barrel contains a **compressible** medium. Pump **displacement** in such cases is much less than for a complete pump fillage and is found from the net or **effective** rather than from the gross plunger stroke length.

The possible reasons for **incomplete** or less than 100% pump fillage are as follows [60]:

- **Gas interference** means that the barrel contains, in addition to liquid, formation **gas** when the plunger reaches its top position at the end of the upstroke. At the start of the downstroke the traveling valve cannot open immediately and it takes part of the downstroke until the gas is **compressed** and the valve opens; pump fillage becomes less than perfect.
- **Fluid pound** happens when there is insufficient **inflow** from the well as compared to the displacement of the downhole pump and the barrel does not fill completely during the upstroke. The upper part of the pump contains a low-pressure gas, the compression of which greatly delays the opening of the traveling valve. Because the traveling valve opens only when the plunger is very close to the liquid level in the barrel, the **impact** of the plunger on the liquid may induce high compression loads in the rod string.
- A **choked or blocked pump** has some restriction at the pump intake that restrains the fluid inflow rate to the barrel during the upstroke, resulting in poor fillage of the pump.

Identification of the possible **causes** of incomplete pump fillage is facilitated by the analysis of the pump card's **shape** and by the results of a **fluid level** survey. As will be shown later, a proper detection of the root cause requires the application of both of these procedures because different problems may create cards of very similar shapes.

Gas Interference

At the start of any discussion on gas interference it must be made clear that the **presence** of gas or a compressible fluid in the barrel affects mainly the **downstroke** portion of the plunger's movement.

Under ideal conditions the traveling valve opens as soon as the downstroke starts because the barrel contains **incompressible** liquid that forces the valve to open. However, a compressible medium in the barrel has to be **compressed** first to a pressure greater than the pressure above the traveling valve so that the valve can open. This kind of operation is explained by the fact that both valves in the pump are simple **check** valves that open and close according to the **balance** of pressures above and below the valve. The result is that part of the plunger's downstroke is used for compressing the fluid in the barrel and does not contribute to the pump's displacement. The loss of displacement is proportional to the portion of the plunger stroke used for compression, i.e., the pump **fillage** defined before.

When modeling the downstroke conditions in the pump one usually assumes a **free** gas phase occupying the top of the barrel space. The behavior of this gas follows the **engineering gas law** while **isothermal** conditions are assumed to prevail because the average temperature in the pump is constant. Although the gas is compressed to quite high pressures during the downstroke, no part of it is **dissolved** in the liquid because of the short time available; the volume of gas at standard conditions, therefore, does not change and is equal to the volume entering the barrel at the pump's suction pressure.

Applying the **engineering gas law** for two conditions—(1) at pump suction where the gas volume occupying the barrel is V_1 and the pressure equals the pump intake pressure, and (2) at any intermediate position of the plunger between the top and the bottom of the stroke where the pressure in the barrel is p_b and the volume available to the gas has decreased to V_2 —one can express the elevated barrel pressure as given in the following expression. Note that solving the formula requires **iterations** because the deviation factor Z_2 is a function of the pressure p_b that is about to be determined.

$$p_b = PIP \frac{V_1}{V_2} \frac{Z_2}{Z_1} \quad (6.44)$$

where:

p_b = pressure in the pump's barrel, psi,

PIP = pump intake pressure, psi,

V_1 = gas volume at suction conditions, cu ft,

V_2 = gas volume at pressure p_b , cu ft,

Z_1 = gas deviation factor at suction conditions, —, and

Z_2 = gas deviation factor at pressure p_b , —.

Knowledge of the compressed gas pressure, p_b , permits the calculation of the variation of plunger **load** versus plunger **stroke** length for the downstroke, i.e., the construction of a part of the pump card. Fluid load on the plunger at any position is found from the **differential** pressure acting on it, as shown here:

$$F_o = A_p (p_d - p_b) \quad (6.45)$$

where:

F_o = fluid load on plunger, lb,

A_p = cross-sectional area of the plunger, sq in,

p_d = pump discharge pressure, psi, and

p_b = compressed gas phase pressure in the barrel, psi.

Pump **discharge** pressure is **constant** during the pumping cycle and equals the pressure at the bottom of the tubing string just above the traveling valve. It is found from the wellhead (tubing head) pressure and the hydrostatic pressure of the liquid in the tubing string:

$$p_d = WHP + 0.433 L_{\text{pump}} SpGr_t \quad (6.46)$$

where:

p_d = pump discharge pressure, psi,

WHP = wellhead (tubing head) pressure, psi,

$SpGr_t$ = specific gravity of the liquid in tubing, $-$, and

L_{pump} = pump setting depth, ft.

Utilizing the equations just discussed, one can completely describe the conditions of pumping a compressible fluid during the plunger's downstroke. Since the pump intake, PIP , and the pump discharge, p_d , pressures are constant, the variation of the pressure in the barrel below the traveling valve, p_b , must be properly estimated to simulate the loads on the plunger.

For illustration purposes a sample case is introduced with the following basic data:

Plunger size = 2 in

Plunger stroke length = 144 in

Pump discharge pressure = 1,600 psi

Pumping temperature = 150 F

Gas specific gravity = 0.6

Pump fillage = 50%

Calculation results are contained in Fig. 6.33, where plunger **loads** during the gas compression are displayed for various pump intake pressure values as a function of plunger **position**. Note that plunger

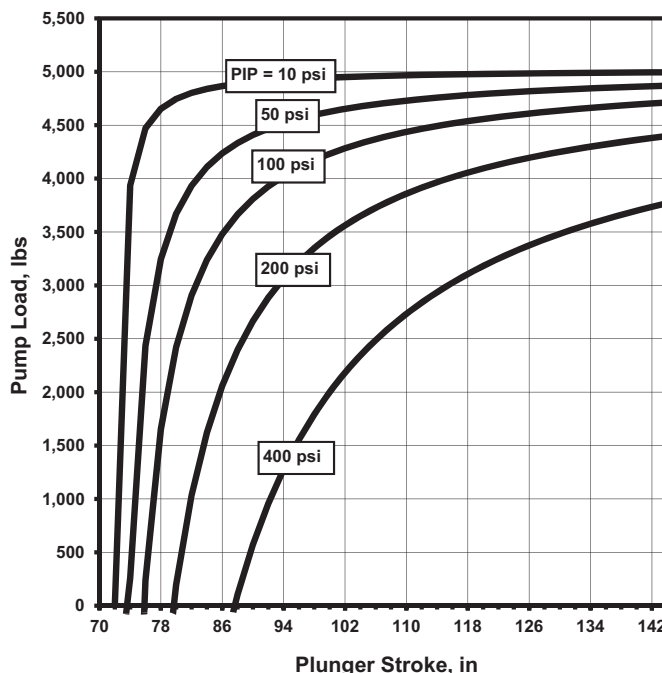


FIGURE 6.33

Calculated pump loads during gas compression for different pump intake pressures.

position is directly proportional to the plunger's swept **volume** because of the constant diameter of the barrel. Plunger loads are found from Eq. (6.45) using the barrel pressures, p_b , calculated from Eq. (6.44) describing the gas compression process.

Curves for each PIP value have characteristic **hyperbolic** shapes typical of gas **compression** processes. The traveling valve opens when the plunger has compressed the gas to a pressure **equal** to the discharge pressure of the pump and the load on the plunger goes down to zero (see Eq. 6.45). As can be seen, higher pump intake pressures require smaller portions of the plunger stroke to compress the gas in the barrel, while for extremely low intake pressures the plunger has to reach down very close to the original liquid level in the barrel.

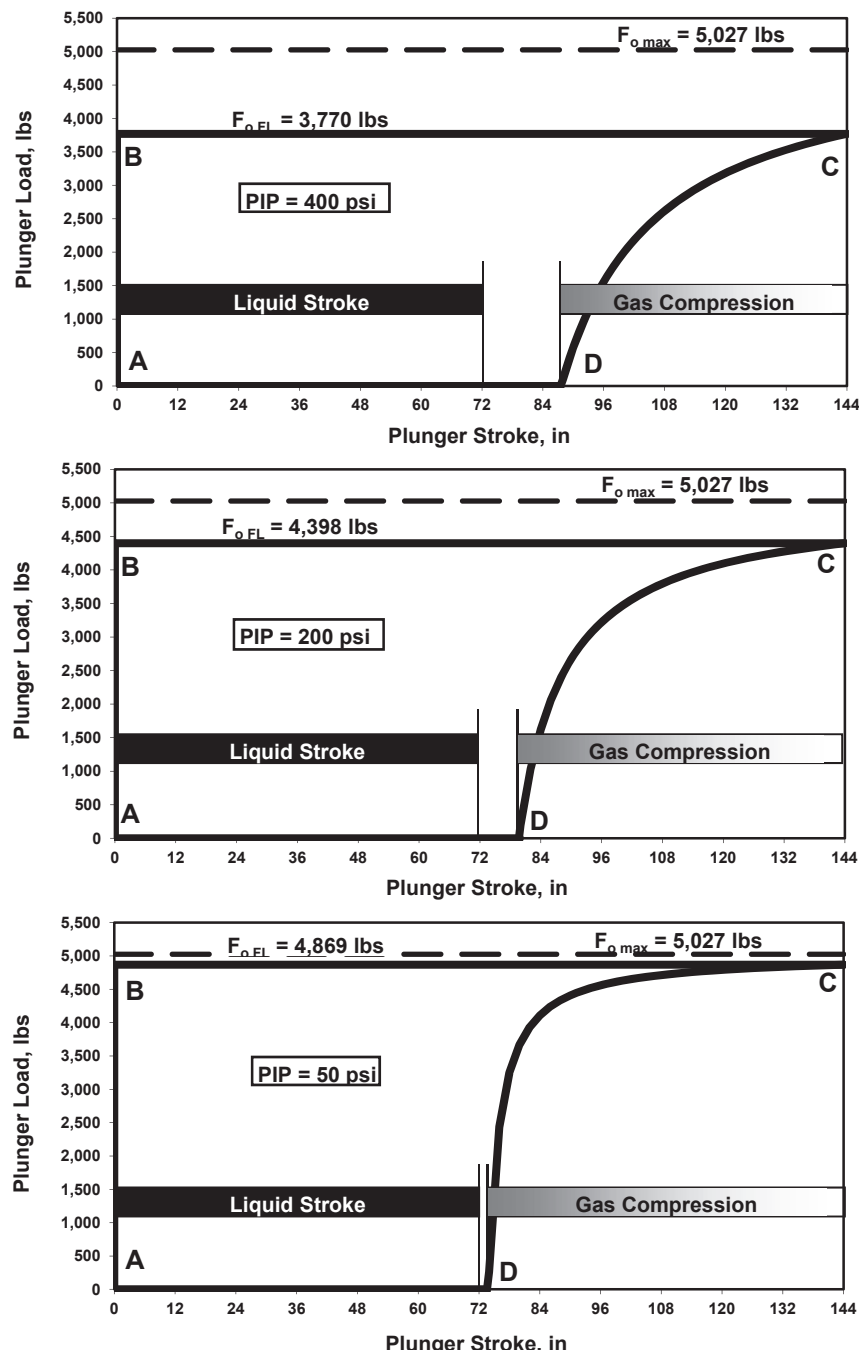
The results of this example allow the construction of **synthetic** pump cards for various cases. This is accomplished by taking one of the curves valid for a given PIP in Fig. 6.33 and constructing the remaining parts of the pump card. The synthetic pump cards prepared for an **anchored** tubing string are given in Fig. 6.34 for various pump intake pressures. The figure also contains the reference lines discussed previously: these are the maximum possible fluid load, $F_{o \text{ max}}$, and the fluid load found from the fluid level, $F_{o \text{ FL}}$, both calculated from the basic formula Eq. (6.45):

$$F_{o \text{ max}} = (2^2\pi)/4(1,600 - 0) = 5,027 \text{ lb; since } PIP = 0.$$

$$F_{o \text{ FL}} = (2^2\pi)/4(1,600 - 400) = 3,770 \text{ lb; since } PIP = 400 \text{ psi.}$$

Let's first describe the sucker-rod pumping cycle for the case with a pump intake pressure of 400 psi. When the upstroke starts at point **A** both valves are closed; now the plunger moves a very short distance and the fluid load is **immediately** transferred from the standing to the traveling valve when the standing valve opens at point **B**. The plunger carries the fluid load $F_{o \text{ FL}} = 3,770$ lb calculated from Eq. (6.45) by substituting $p_b = PIP$. The immediate opening of the standing valve from point **A** to point **B** happens only if the pump has a small **dead space**; then a very small movement of the plunger can sufficiently decrease the pressure in the barrel to the level of the pump intake pressure. Otherwise, especially if the pump is spaced too high, the opening of the standing valve is **delayed** and point **B** moves horizontally to the right.

The barrel is filling up with a mixture of gas and liquid during the plunger's travel from point **B** to point **C**. At point **C** (the top of the plunger's stroke) the barrel is full with a multiphase mixture whose pressure is at the pump intake pressure, $p_b = PIP$. From point **C** the **downstroke** starts and the plunger descends with a still-closed traveling valve continuously increasing the pressure inside the barrel. The gas contained at the top of the barrel is **compressed** from point **C** to point **D** and the pressure below the traveling valve progressively increases. Close to point **C** but farther on the downstroke, the increased pressure forces the standing valve to close. The load on the plunger decreases simultaneously with the increased barrel pressure because load is found from the differential pressure across the plunger (see Eq. 6.45). As soon as gas pressure reaches the pump discharge pressure of 1,600 psi at point **D** (at a plunger stroke length of 87.5 in) the traveling valve opens. The plunger with the open traveling valve now moves down in the compressed gas until it reaches the liquid at a stroke length of 72 in, which is 50% (the original fillage value) of the total stroke length of 144 in. From this position on, the plunger moves in liquid and reaches the bottom of its stroke at point **A**. The **effective** plunger stroke that defines the pump **displacement** is the length of the downstroke while the plunger moves in liquid, which is 72 in in this case. As seen from the relatively high PIP value as well as from the great

**FIGURE 6.34**

Synthetic pump cards for an anchored tubing string and different pump intake pressures.

difference between the $F_o \text{ max}$ and the $F_o \text{ FL}$ reference lines, the annular liquid level is well above the pump setting depth.

Comparison of the pump cards valid for the different cases given in Fig. 6.34 shows that fluid load during the upstroke, $F_o \text{ FL}$, increases and approaches the possible maximum load $F_o \text{ max}$ as the pump intake pressure decreases. This indicates that the liquid level in the annulus drops toward the pump. It is also interesting to note that the actual liquid **fillage** of the pump is not at point **D** where the traveling valve opens but always at a lower position. As clearly seen from the figures, the difference is greater at higher *PIP* values and is negligible for extremely low *PIPs*. A general **conclusion** for pump card diagnosis is that at higher *PIPs* the plunger's **effective** stroke length is less than the value estimated from the plunger position at the opening of the traveling valve.

The most important problem with gas interference is the **reduction** of effective plunger stroke length and the associated **loss** of liquid production. Additional troubles are related to the pump's reduced **speed** at the downstroke when the fluid is compressed in the barrel. As the pump slows down, rods above it that were falling at a high speed now go into **compression** and start to **buckle**; the tubing and the rods are damaged. Couplings on the rods may loosen, leading to pin failures; all these difficulties are eliminated if a properly sized gas separator is used to maintain a high liquid fillage of the pump.

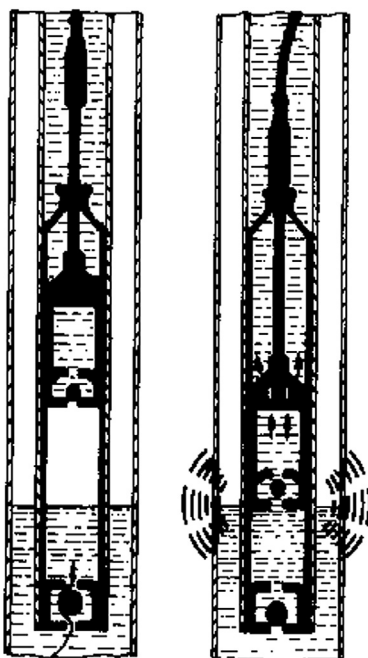
Fluid Pound

Fluid pound condition is experienced when the lifting capacity of the pump **exceeds** the liquid inflow rate to the well and the pump barrel is not completely filled with liquid by the time the plunger reaches its upstroke. The fluid level in the annulus is at the pump intake, as seen in Fig. 6.35, and the barrel space above the liquid is occupied by low-pressure **gas** sucked in from the annulus. This situation is very **similar** to the gas interference problems described previously, with the only difference that very **low** pump intake pressures are involved; gas interference and fluid pound, therefore, can be **distinguished** on the basis of the actual pump intake pressure.

The description of the pumping cycle, because of the great **similarity** to gas interference problems, follows that detailed previously. Figure 6.36 presents a **synthetic** pump card prepared for the same case as before but using a very low pump intake pressure of *PIP* = 10 psi. As seen, the plunger load calculated from the fluid level, $F_o \text{ FL} = 4,995 \text{ lb}$, is almost identical to the maximum possible fluid load of $F_o \text{ max} = 5,027 \text{ lb}$, valid at zero pump intake pressure. This indicates that the liquid level in the annulus is at the pump intake; the well is being **pumped off**. The transfer of the fluid load from the traveling to the standing valve is very late in the downstroke and it takes half of the 144-in stroke length of the plunger to compress the low-pressure gas occupying the barrel. Pump **fillage**, as read at point **D**, is identical to the fraction of liquid in the barrel at the end of the upstroke, 50%.

The opening of the traveling valve at point **D** happens just **before** the plunger reaches the liquid level in the barrel; for the example case calculations similar to those presented before give a distance of about 0.5 in between the plunger and the liquid before impact. This means that, contrary to previous theories, the plunger hits the liquid with an **open** traveling valve [61] and never with a closed one; impact forces, therefore, are much smaller than those a closed traveling valve would cause. Most of the time these impact forces do not even show up on the pump card, so they cannot cause rod compression and buckling problems at the bottom of the rod string, contrary to previous beliefs.

Fluid pounding, however, causes compressive forces and may induce buckling of the rod string **above** the plunger; this can be explained from an analysis of plunger **velocity** during the gas



UPSTROKE DOWNSTROKE

FIGURE 6.35

Illustration of pump action for fluid pound conditions.

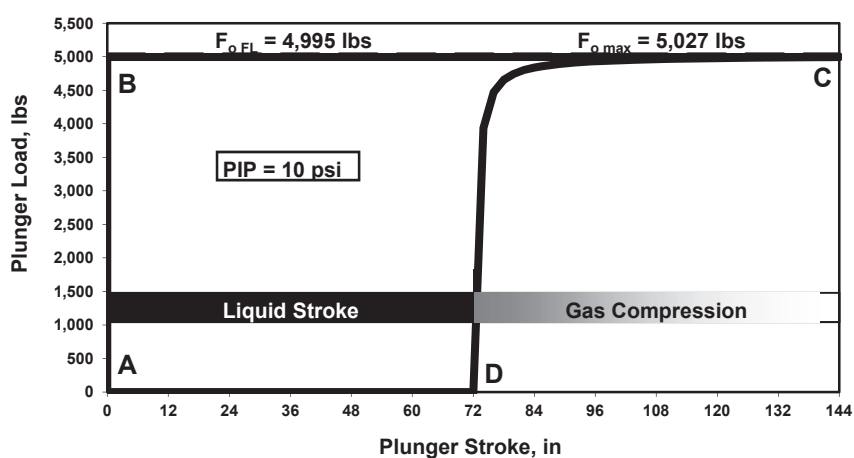


FIGURE 6.36

Synthetic pump card for pumped-off conditions.

compression period. At the beginning of this period at point **C** plunger velocity approximates the velocity of the polished rod, but it rapidly **decreases** as the plunger nears the liquid level in the barrel and compresses the gas above the liquid. The plunger may even **stop** moving for a short time when reaching the liquid level in the barrel as the traveling valve opens at around point **D**. Thus, while the rest of the rod string falls with a high velocity the bottom part of it is almost stopped; the great velocity difference causes compressive forces in the elastic rod material. The compressive forces thus generated may cause **buckling** in the rod string above the downhole pump. It is important to note that these compressive forces cannot usually be detected on the pump card; only the variation of **effective loads** along the rod string gives a proper indication [62].

As seen in Fig. 6.36, a fluid pound is often clearly indicated by the **shape** of the pump card. Its characteristic feature is the very **steep drop** in plunger loads well after the start of the downstroke, which occurs deeper and deeper in the downstroke as the fluid pound gets more and more severe during consecutive strokes. Another characteristic feature is the **pumped-off** condition: the liquid level in the annulus being at the pump intake, the fluid load on the plunger is close to the maximum possible value, $F_o \text{ max}$, indicating a **low** pump intake pressure.

The dynamic loads occurring during fluid pounding can have several **detrimental** effects on the downhole equipment: the rod string can experience helical **buckling** leading to rod breaks, rod-to-tubing **wear** is increased, shock loads contribute to coupling **failure** due to unscrewing, and pump parts can be damaged, as well as the tubing, if unanchored. Dynamic loads are transmitted to the surface across the rod string and can reach the polished rod; hence the name **fluid pound**.

Choked Pump

In some cases, although a sufficiently high liquid column exists above the pump intake the pump operates with a very **low** liquid fillage. This kind of operation is caused by a **restricted** inflow into the pump barrel that prevents the barrel from filling up completely by the end of the plunger's upstroke. The flow of well fluids may be restricted (**choked**) by **solid** materials such as paraffin, scale, trash, and sand **plugging** the pump intake and/or the standing valve, and the pump is starved of liquid. Pumping of a highly **viscous** crude causes similar problems because the high frictional pressure losses across the standing valve and the pump intake may greatly reduce the liquid rate into the pump. Plunger displacement, therefore, may **exceed** the inflow rate, and as a result the barrel is only **partially** filled during the upstroke. The liquid volume filling up the barrel comes from two sources: from the annulus, and from the tubing through slippage in the barrel-plunger fit and/or from traveling valve leaks. Thus, in a completely blocked pump when no liquid reaches the wellhead, the only liquid in the barrel is due to slipping and leaking from the tubing.

As a result of choked inflow into the pump, the **pressure** below the plunger is extremely **low**. In case of a total **blockage** it can go down to the vapor pressure of the crude valid at ambient temperature; otherwise, it is normally close to **atmospheric** pressure. Due to this low pressure below the plunger, the pump load during the upstroke (see Eq. 6.45) is very high; it usually reaches $F_o \text{ max}$, the maximum fluid load belonging to a **pumped-off** condition. Thus, although there is a sufficient amount of liquid in the annulus the pressure below the plunger is very low.

As the downstroke starts, the plunger falls with the **closed** traveling valve in the barrel containing an extremely low pressure gas. Since there is not much gas to be compressed, the traveling valve cannot open before **hitting** the liquid level; the impact produces great **compression** forces at the bottom of the sucker-rod string. The resulting vibrations force the traveling valve to open and close

rapidly several times before the valve finally opens and reaches the bottom of the stroke in the liquid. So, in contrast to the usual conditions during **fluid pounding**, the plunger hits the liquid level with a **closed** traveling valve, causing rod **buckling** and **damage** to the pump as well as the tubing string.

The general shape of the pump card is displayed in Fig. 6.37, representing a **synthetic** card for choked pump conditions with an **anchored** tubing string. The fluid load calculated from the fluid level, $F_o FL$, represents the conditions for the relatively high **PIP** value corresponding to the liquid column existing in the annulus. Since the actual pressure below the plunger, due to the restricted inflow to the barrel, is much lower than the **PIP**, plunger loads during the upstroke are greater and close to $F_o max$. This is exactly what is observed in **fluid pound** conditions when there is not enough inflow from the well; but now there is a sufficient liquid column in the annulus. The contradiction is explained by the fact that the choked pump creates a great pressure drop across the pump intake.

As can be seen by comparing Fig. 6.37 to Fig. 6.36, pump cards for a **choked pump** are very similar to cards found in **pumped-off** conditions. Proper diagnosis of the case is only possible if, simultaneously to the dynamometer measurements, a **fluid level** survey is also made to detect the dynamic liquid level in the well's annulus; a **high** liquid level is a positive indication for restrictions at the pump intake. Another sign for a choked pump could be the relatively high **negative** load caused by the plunger hitting the liquid level in the pump barrel during the downstroke. When hitting the liquid, the plunger's **velocity** decreases dramatically and the plunger may even **stop** for a short period. Then, just like in fluid pound conditions, the rod string experiences high **compressive** forces, leading to helical **buckling** and severe operational problems.

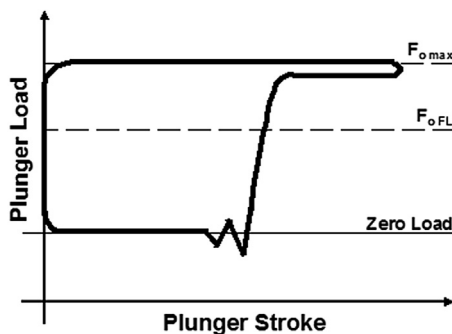


FIGURE 6.37

Synthetic pump card for a choked (blocked) pump.

6.4.2.3.2 Unaccounted friction

Let's start with the definition of **unaccounted** friction: any kind of friction along the rod string that is not accounted for during the solution of the damped wave equation. As discussed in Chapter 4, the conventional wave equation includes energy losses of a **viscous** nature only and cannot calculate any losses except those due to **viscous damping** that take place between the rod string and the well fluid. However, mechanical (a.k.a. Coulomb) **friction** occurs in the polished rod as it moves inside the stuffing box, between the rods and the tubing, etc. The effect of Coulomb friction is especially important in **deviated** wells where rod-tubing friction may become dominant; treatment of such cases requires the **modification** of the wave equation.

Since the **diagnostic** analysis of surface dynamometer cards is normally accomplished by using the conventional wave equation, cases with **negligible** Coulomb friction along the rod string give **reliable** results and the calculated pump cards are fully representative. The effect of increased mechanical friction in the well is clearly indicated in the calculated pump card: pump loads increase because the wave equation cannot remove all energy losses (viscous plus friction) from the power introduced at the polished rod. A **synthetic** pump card (for a perfect pump and an anchored tubing string) is shown in Fig. 6.38, where the typical symptoms of unaccounted friction are clearly indicated: downstroke loads are negative, upstroke loads are higher than normal, and the load range is excessive. Normal pump loads (**effective** loads) should fall between zero and the fluid load $F_o FL$ calculated from the pump intake pressure, which, in turn, is found from the dynamic liquid level. Cards with loads outside this range clearly indicate that the conventional wave equation is not able to **remove** all downhole losses from the pumping system; calculated pump loads are increased by the **unaccounted** friction loads.

Possible **sources** of unaccounted friction may include the following:

- Well **deviation** is the prime source of mechanical friction along the rod string; highly deviated wells cannot be diagnosed with the conventional wave equation.
- An **overtightened** stuffing box generates extra load on the polished rod; this can be detected on the surface dynamometer diagram if vertical changes in load are observed at the start and the end of the polished rod's stroke.
- **Deposition** of paraffin, scale, etc. on the rod or tubing.
- Friction in the **pump** due to a bent or sticking barrel.

Another effective way to detect unaccounted friction is the analysis of **valve tests**. In these cases the measured loads for the traveling and the standing valve tests are greater and respectively lower than under normal conditions due to the friction forces working opposite the direction of movement. If the plot of the traveling valve load versus time is investigated, then a definite **drop** in load can be observed some time after the unit is **stopped**. At this point the frictional load felt by the polished rod during the upstroke is released because the rod string's movement ceases.

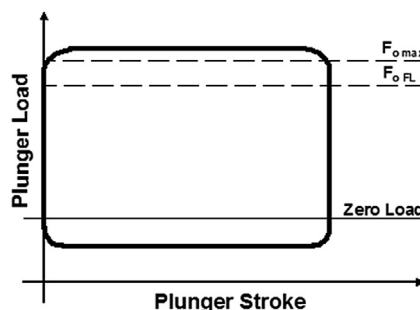


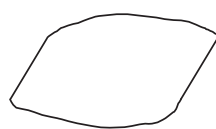
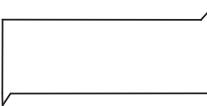
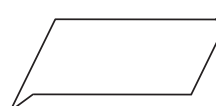
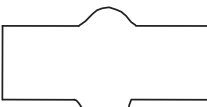
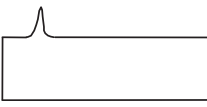
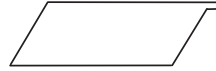
FIGURE 6.38

Synthetic pump card showing unaccounted friction.

6.4.2.3.3 Typical synthetic pump cards

Different downhole problems **distort** the shape of the ideal pump card in different but usually **typical** ways. Some possible **synthetic** pump card shapes are given in [Table 6.1](#), which display pump cards for **anchored** and **unanchored** tubing strings for the equipment malfunctions and downhole pump problems listed. These shapes allow the **identification** of the actual pumping difficulty if caused by a

Table 6.1 Possible Synthetic Pump Card Shapes for Anchored and Unanchored Tubing Strings

Anchored Tubing	Description	Unanchored Tubing
	Ideal card Pump properly functioning completely filled with liquid.	
	Full pump with unaccounted friction Extra friction along the rod string is not removed by the wave equation used to calculate the pump card.	
	Plunger tagging Plunger hits up or down because of improper spacing of the pump.	
	Tubing anchor slipping Malfunctioning tubing anchor allows tubing to stretch.	
	Bent or sticking barrel Load increases on upstroke, decreases on downstroke in defective section of barrel.	
	Worn or split barrel Rod load decreases in defective section of the barrel.	
	Sticking plunger Load spike shows where plunger stopped; extra load is needed to overcome friction in the pump at this position.	
	Slight fluid pound Fluid level falling to pump intake.	

Continued

Table 6.1 Possible Synthetic Pump Card Shapes for Anchored and Unanchored Tubing Strings—cont'd

Anchored Tubing	Description	Unanchored Tubing
	Severe fluid pound Barrel incompletely filling with liquid due to limited well inflow.	
	Well pumped off Pump displacement much greater than well inflow. PIP, pump fillage are low.	
	Gas interference Mixture of liquid/gas fills barrel. PIP is high, pump fillage is low. Unstable operation.	
	Gas-locked pump Barrel filled with gas, valves remain closed, no liquid production. Low PIP.	
	Choked pump Intake plugged, barrel incompletely fills during upstroke. PIP is high, pump fillage is low.	
	Leaking TV or pump TV leak or pump slippage causes delay in picking up and premature unloading of fluid load.	
	Badly leaking TV or pump TV or plunger/barrel completely worn out.	
	Leaking SV Premature loading at start of upstroke and delayed unloading at start of downstroke.	
	Badly leaking SV SV completely worn out.	
	Worn-out pump TV & SV valves and barrel/plunger completely worn out.	
	Delayed closing of TV TV ball does not seat as soon as upstroke starts.	
	Hole in barrel or plunger pulling out of barrel Load drops as plunger reaches hole or pulls out.	

single problem only; cases with multiple problems have shapes combined from individual typical shapes. Once again, troubleshooting downhole pumping problems is much easier using pump cards than surface dynamometer cards because pump cards have more uniform and more easily recognizable shapes.

6.4.2.3.4 Cards in special cases

When diagnosing sucker-rod pumping installations, one often finds cases with **no fluid** production reaching the surface. The surface and pump dynamometer cards obtained on such wells have very specific **features** from which the actual downhole problems can be identified. The following discussions, after [60], describe the **six** different possible situations by presenting **typical** surface and pump cards along with their diagnosis. Proper identification of the existing downhole problems is facilitated by the use of the **reference lines** plotted on the surface and pump cards, as described in **Section 6.4.2.2**. It must be noted that dynamometer surveys for the six cases investigated have to be made using **horseshoe** transducers because PRTs always force the bottom of the pump card to lie on the **zero** load line. Additionally, the pump card must be plotted using **effective loads** because the use of true loads prevents a proper diagnosis in some of the investigated cases.

Deep Rod Part

In case the rod string breaks at or very close to the pump setting depth, or if the valve rod in the pump is broken, then the plunger and the rod string are **separated** and no pumping action is performed. The pump card lies on the zero load line and is very **flat** because the bottom of the string is not loaded (see **Fig. 6.39**). The polished rod loads as read from the surface dynamometer card are close to the buoyant **weight** of the rod string, W_{rf} , since there is no fluid load applied by the pump to the rod string. The surface card shape is similar to an **overtravel** card with the usual downward slope to the right.

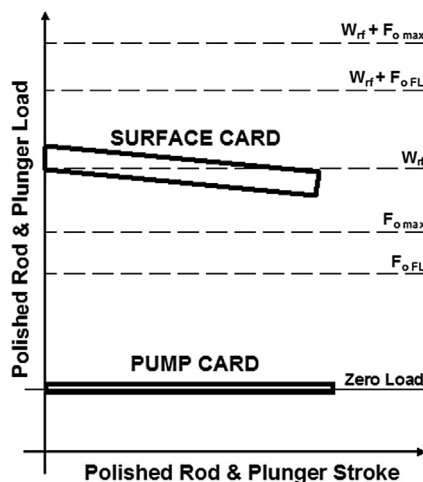


FIGURE 6.39

Surface and pump cards typical for a deep rod part.

Overtravel conditions occur because of the lack of rod string stretch due to the missing fluid load, and downhole stroke length becomes longer than the polished rod stroke. Note that a traveling valve stuck open during the pumping cycle produces exactly the same symptoms as described here because the rod string and the plunger are no longer attached to each other (see later).

Shallow Rod Part

The conditions with a rod break situated high above the pump are described in Fig. 6.40. Surface loads are less than the calculated buoyant rod string weight, W_{rf} , because the lower part of the string is missing. The very flat pump card is **shifted** below the zero load line by exactly the buoyed weight of the missing rod sections. This fact permits the determination of the **depth** of the rod break in the knowledge of the original taper lengths. To do so one has to repeat the calculation of the downhole card by **removing** different assumed lengths from the bottom of the rod string. The proper length of the broken string is found when the new pump card lies around the zero load line.

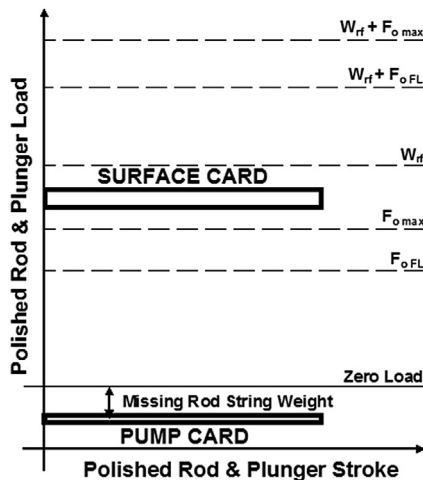
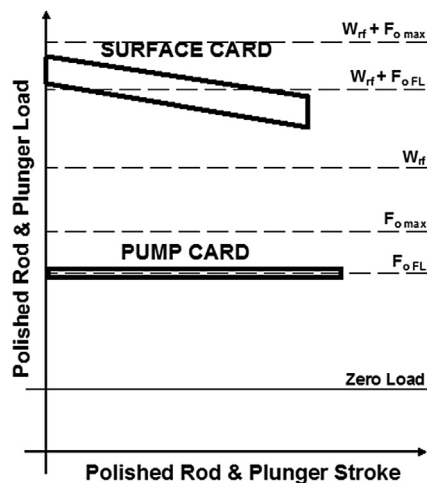


FIGURE 6.40

Surface and pump cards typical for a shallow rod part.

Standing Valve Stuck Open

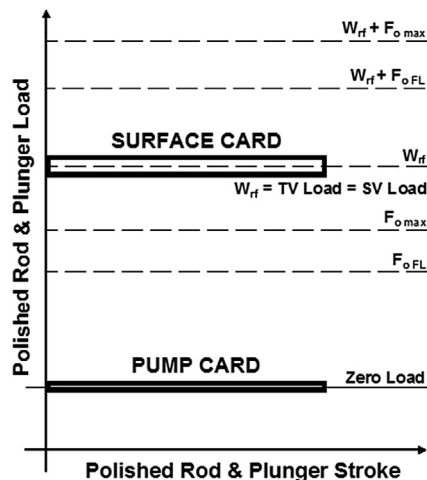
The standing valve of the downhole pump may be kept open by some foreign material (scale, sand, trash, asphaltene, etc.) that causes its ball to **stick** in the valve cage; or keeps it off the valve seat. This condition prevents the **transfer** of the fluid load from the traveling valve to the standing valve during the downstroke. Polished rod loads, therefore, do not considerably change at the downstroke (see Fig. 6.41); the surface card may exhibit slight overtravel. Since the traveling valve **never** opens, polished rod loads are close to the sum of the buoyant weight of the string plus the fluid load, $W_{rf} + F_{o\ FL}$. The pump card is flat because the plunger carries the fluid load during both the up- and the downstroke; it lies on the load that can be calculated from the fluid level in the annulus, $F_{o\ FL}$.

**FIGURE 6.41**

Surface and pump cards typical for a standing valve stuck open.

Traveling Valve Stuck Open

Just like in the standing valve, the ball of the traveling valve may **stick** in the cage or may be kept from closing on the valve seat by **foreign** material such as trash, sand, and asphaltene. Since there is no pumping action due to the permanently open traveling valve, pump loads are close to **zero** and the pump card lies around the zero load line (see Fig. 6.42). The loads on the surface dynamometer card

**FIGURE 6.42**

Surface and pump cards typical for a traveling valve stuck open.

are approximately equal to the buoyant rod string weight, W_{rf} . Under these conditions, testing of the pump's valves gives identical loads for the **TV test** and **SV test**; both are equal to the buoyant rod string weight, W_{rf} .

The symptoms of a stuck traveling valve are very similar to those observed in a deep rod part condition (see Fig. 6.39) because in both cases the connection between the rod string and the plunger is lost. A stuck traveling valve may be **cleared** by lightly **tagging** the plunger on the downstroke, whereas a parted string does not react to such an operation.

Blocked Pump Intake

The intake to the downhole pump may be partially or completely **choked off** by solids such as sand, scale, trash, and asphaltene and inflow to the pump barrel may become **restricted** or completely **blocked**. Blockage may also be caused by a sand screen **clogged** with fines or the pump intake may be covered by sand when the pump is set below the perforations. The common result of these problems is that the barrel does not fill with liquid during the upstroke or can even become empty. Due to the blocked intake the **pressure** inside the barrel during the upstroke goes down to zero and the plunger carries a load much higher than the load calculated from the measured fluid level, $F_o FL$, as shown in Fig. 6.43. The flat pump card, therefore, lies very close to the **maximum** possible fluid load, $F_o max$. The surface card, too, shows a relatively constant load equal to the sum of the buoyant rod string weight and the maximum possible fluid load, $W_{rf} + F_o max$.

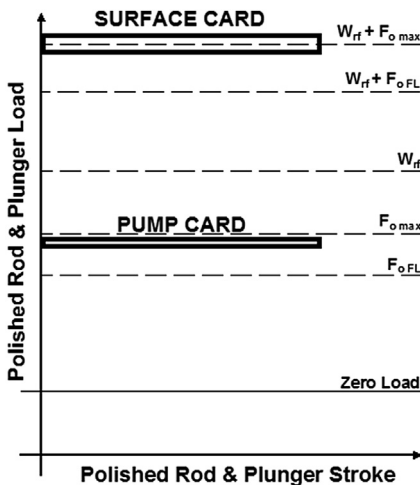


FIGURE 6.43

Surface and pump cards typical for a blocked pump intake.

Deep Hole in Tubing

If the tubing string has a hole at a relatively **deep** position, then the liquid produced by the pump is **circulated** through that hole back to the annulus. The pump, if in a good overall condition, does considerable work and the pump card is not as flat as in the other cases that do not produce fluid to the surface (see Fig. 6.44). If the tubing leak is big enough, the tubing above the depth of the hole is

practically **dry**. Due to this fact, the measured **weight** of the rod string considerably **increases** because most of the string operates in air; the buoyancy force for the dry section is missing. The pump card, therefore, is **shifted** above the zero load line by the load equal to the **missing** buoyancy force. Fluid load on the plunger, as compared to previous cases, is considerably **greater** but much lower than normal because the pump lifts liquids up to the tubing leak only. The surface card, similarly to the pump card, is not flat and is situated above the buoyant rod string weight, W_{rf} .

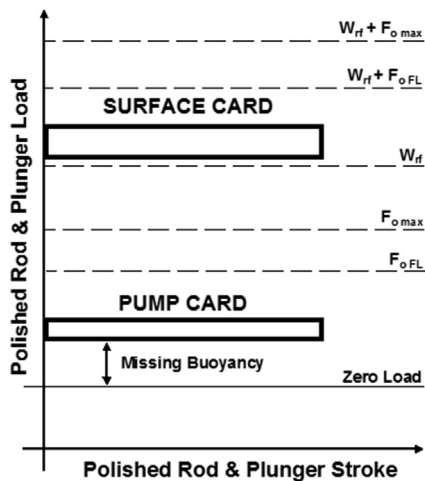


FIGURE 6.44

Surface and pump cards typical for a deep hole in the tubing.

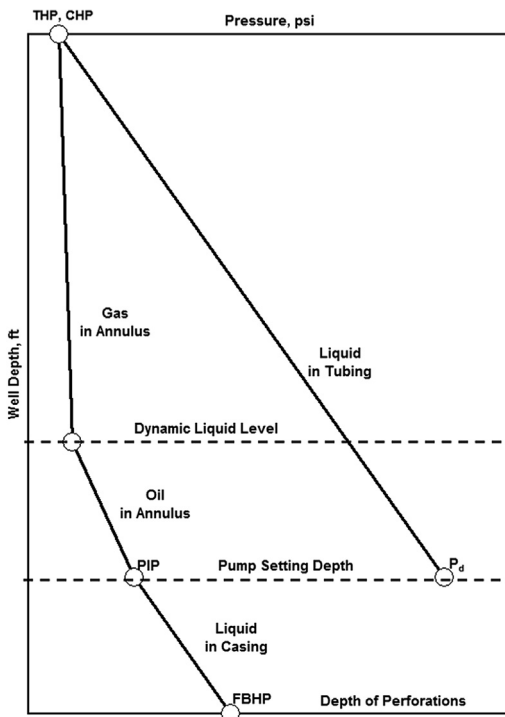
6.4.2.4 Pump intake pressure calculations

The actual pressure valid at the downhole pump's suction level is called the **pump intake pressure** or **PIP**, which is an important parameter for the evaluation of pumping conditions. One can, for example, use the **PIP** to detect the existence of any **free** gas at the pump suction by calculating the amount of gas in solution in the produced oil. The actual value of **PIP** also indicates the depth of the dynamic liquid **level** present in the well's annulus, which, in many cases, is not directly measured. Calculation of the pump intake pressure, therefore, is a standard procedure and the three different ways of its execution are detailed in the following [63,64]. As will be seen, all methods have different **accuracies** and reliabilities and require different input data. It must be noted that the analyst must not accept the result of a **single** calculation model but must use as many of them as possible so that, by comparing all results to any other available evidence, a **verified** **PIP** value can be selected.

6.4.2.4.1 Using acoustic survey data

As already discussed in [Section 6.2.3.3](#), **PIP** (the fluid pressure at pump suction level) is made up of **three** components, as displayed in [Fig. 6.45](#):

- the well's **casinghead** pressure,
- the pressure of the static **gas column** present in the annulus, and
- the pressure of the **gaseous liquid** (in stabilized wells, pure oil) column above the pump.

**FIGURE 6.45**

Pressure distributions in a pumping well's annulus and in the tubing string.

Of the components presented, the determination of the pressure of the gaseous oil column situated in the well's annulus is **critical** and the iterative procedure detailed in [Section 6.2.3.3.1](#) is applied. Considering the calculation and measurement accuracy of the relevant terms, average *PIP* calculation **errors** (as compared to data received from downhole pressure recorders) of less than 5% can be expected according to **Rowlan et al.** [64]. This accuracy is valid for **stabilized** production conditions and consistent input data. Of the three possible procedures for finding *PIPs*, the use of acoustic survey data is the most **reliable** and most **accurate** one.

EXAMPLE 6.10: FIND THE PUMP INTAKE PRESSURE FOR THE FOLLOWING CASE WHEN THE WELL PRODUCES A NEGLIGIBLE AMOUNT OF GAS

$$\text{Pump setting depth} = 6,500 \text{ ft TVD}$$

$$\text{Oil } SpGr = 0.85$$

$$\text{Measured liquid level} = 5,000 \text{ ft TVD}$$

$$\text{Gas } SpGr = 0.65$$

$$\text{Casinghead pressure} = 300 \text{ psi}$$

Solution

The gas gradient in the annulus at the given casinghead pressure is found from Appendix A as 7.5 psi/1,000 ft; the gas pressure at the measured liquid level is found from this and the casinghead pressure:

$$p_g = 300 + 7.5 \times 5,000 / 1,000 = 37.5 \text{ psi.}$$

The hydrostatic pressure of the gasless oil column above the pump is found as:

$$p_l = (6,500 - 5,000) \times 0.433 \times 0.85 = 552 \text{ psi.}$$

Pump intake pressure is the sum of the calculated pressures:

$$PIP = 37.5 + 552 = 587.5 \text{ psi.}$$

6.4.2.4.2 Based on valve test results

As discussed previously, when testing the valves of a downhole pump with **perfectly** operating valves, the loads measured at the onset of the tests are as follows. The **TV test** gives an initial load equal to the sum of the buoyant **weight** of the rod string and the **fluid load**:

$$TV \text{ Load} = W_{rf} + F_o \quad (6.47)$$

The **SV test**, on the other hand, furnishes the buoyant **weight** of the rod string only:

$$SV \text{ Load} = W_{rf} \quad (6.48)$$

where:

TV Load = load measured at the **TV test**, lb,

SV Load = load measured at the **SV test**, lb,

W_{rf} = buoyant rod string weight, lb, and

F_o = fluid load on the plunger, lb.

From these two expressions the **fluid load** on the plunger can be easily determined, valid for conditions with negligible **leakage** in the pump's valves and no unaccounted **friction** in the pumping system:

$$F_{o \text{ VT}} = TV \text{ Load} - SV \text{ Load} \quad (6.49)$$

where:

F_o VT = fluid load calculated from valve test data, lb.

The fluid load on the plunger, *F_o*, however, can also be expressed based on the cross-sectional **area** of the plunger, *A_p*, and the **differential** pressure acting on the plunger. The pressure **above** the plunger (the pump's discharge pressure, designated *p_d* in Fig. 6.45) comes from the wellhead (tubing head) pressure and the hydrostatic pressure of the produced liquid, as shown in the same figure. Since the pressure **below** the plunger is equal to the pump intake pressure, *PIP*, one can write:

$$F_o = A_p (WHP + 0.433 SpGr_t L_{\text{pump}} - PIP) \quad (6.50)$$

where:

F_o = fluid load on the plunger, lb,

A_p = cross-sectional area of the plunger, sq in,

WHP = wellhead (tubing head) pressure, psi,

$SpGr_t$ = specific gravity of the liquid in tubing, –,

L_{pump} = true vertical pump setting depth, ft, and

PIP = pump intake pressure, psi.

Expressing PIP from this equation and substituting F_o VT from Eq. (6.49), we get the final formula for the calculation of the pump intake pressure utilizing valve test data:

$$PIP = WHP + 0.433 SpGr_t L_{\text{pump}} - \frac{TV \text{ Load} - SV \text{ Load}}{A_p} \quad (6.51)$$

where:

PIP = pump intake pressure, psi,

WHP = wellhead (tubing head) pressure, psi,

$SpGr_t$ = specific gravity of the liquid in tubing, –,

L_{pump} = true vertical pump setting depth, ft,

$TV \text{ Load}$ = load measured at the **TV test**, lb,

$SV \text{ Load}$ = load measured at the **SV test**, lb, and

A_p = cross-sectional area of the plunger, sq in.

A comprehensive study [64] on the use of this method reported average calculation errors of $\pm 10\%$, compared to data received from downhole pressure gauges. However, of the three models available for PIP calculations, this is the **least** reliable and accurate; the low reliability is caused by the many possible errors if valve test procedures are not followed correctly.

6.4.2.4.3 Using the pump card

The previous procedure used **static** loads on the plunger for the calculation of PIP values. If **dynamic** loads are considered then one can use the loads read from the downhole card received from the solution of the damped **wave** equation. Proper estimation of the average up- and downstroke loads on the plunger, as discussed in Section 6.4.2.2 permits the estimation of the pump intake pressure based on those F_{UP} and F_{DWN} loads. By substituting these loads in Eq. (6.51) we get:

$$PIP = WHP + 0.433 SpGr_t L_{\text{set}} - \frac{F_{\text{UP}} - F_{\text{DWN}}}{A_p} \quad (6.52)$$

where:

PIP = pump intake pressure, psi,

WHP = wellhead (tubing head) pressure, psi,

$SpGr_t$ = specific gravity of the liquid in tubing, –,

L_{set} = true vertical pump setting depth, ft,

F_{UP} = estimated average plunger load on the upstroke, lb, and

F_{DWN} = estimated average plunger load on the downstroke, lb.

The calculation model relies heavily on the accuracy of **solving** the damped wave equation because the loads F_{UP} and F_{DWN} are read from the calculated downhole card. Since the shape and scale of the pump card depend on the assumed **damping factor**, proper estimation of the damping factor is

important. Another limitation is that accurate *PIP* data are received only in cases when there are negligible **unaccounted** friction forces during the pumping cycle. This procedure is considered to be more **reliable** than the one using valve test data but less accurate than the method based on acoustic surveys.

The merits of this procedure were investigated by **Pons et al.** [65] by comparing measured *PIPs* to values calculated with the help of the solution of the damped wave equation; for over 77% of nine cases the differences were below 30 psi.

6.4.3 MODERN INTERPRETATION METHODS

In analyzing surface or pump cards as well as in diagnosing pumping problems, the need for expert **knowledge** is essential. Only a person long experienced in rod-pumping analysis can be expected to properly and reliably interpret most dynamometer cards. Since expert knowledge is usually rare, the latest trend in dynamometer card analysis methods aims at reducing the **dependence** on human expertise by applying the methods of **artificial intelligence** (AI). The most commonly applied AI method in dynamometer card analysis is the use of **expert systems**, which are computer programs that simulate the problem-solving process of a human. They are based on detailed knowledge gained from rod pumping **experts** that is stored in computer memory and used in logical **decisions** that lead to the interpretation of pump cards. The diagnosis process starts with computer-generated questions to the user, then proceeds with the user's answers; finally, recommendations are given by the program based on the information input and the logic rules previously determined from a human expert's knowledge [66].

In analyzing dynamometer cards with the computer, one of the crucial problems is how the computer can be taught to **recognize** the shape of the card. To solve this, another field of AI is utilized: **pattern recognition**. One possible way to recognize different card shapes is by the use of **templates** previously set up. The templates are constructed according to the characteristic features of the different pumping problems to be detected. One such template to determine fluid pounding conditions [67] is reproduced in Fig. 6.46 with a dynamometer card on it. The card, as shown, is previously transformed into a dimensionless form, and the degree of **matching** is determined on the basis of the **number** of intersections between the card and the template. After all available templates have been used to match

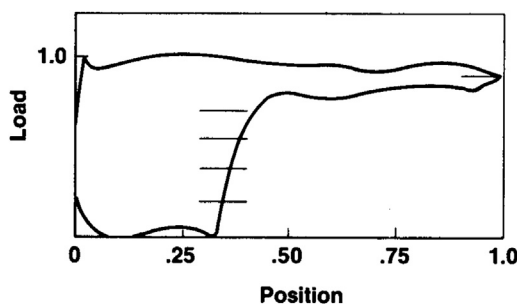


FIGURE 6.46

Use of a template in pattern recognition of pump cards, after **Foley and Svinos** [67].

the actual card, the template with the highest degree of match can be selected. Then, by applying logic rules built into the program, the computer gives a detailed **diagnosis** of the actual card.

The different pattern recognition methods used in dynamometer card analysis are compared by **Dickinson and Jennings** [68]. Another method involves a vector of load and position data derived from the pump card [69,70]. The card, after being transformed into a nondimensional form, is digitized with a sufficient number of points using a constant position increment. These data constitute the components of a **vector** that, after normalization, is claimed to fully **represent** the original card. The diagnosis is based on a comparison of the actual card's vector to data of cards with **known** problems contained in the program's library. The degree of **match** is defined as the dot product of the actual and the library vectors. After the library card with the highest level of match is found, the actual card is easily diagnosed.

The use of an artificial neural network (ANN) to pump card analysis has two modes: learning and retrieving. In the learning mode, pump cards with different problems are input; cards are first normalized, then 80 points and several slopes on the card are read. The many cards input into the system are classified into 11 problem conditions. The ANN program developed [71] could correctly detect the 11 problems and any of their combinations from test cards.

REFERENCES

- [1] Dugan L, Howard L. Beyond pump-off control with downhole card well management. Proc. 49th annual southwestern petroleum short course. Lubbock. Texas. 2002. p. 55–61.
- [2] Boyer L, Gibbs S, Nolen K, Cordoba A, Roberson A. Well production testing using a rod pump controller. Lufkin Automation; 2006. 8 p.
- [3] Gibbs SG, Nolen KB. Inferred production rates of a rod pumped well from surface and pump card information. US Patent 7,212,923; 2007.
- [4] Ahmed M, Sadek N. Automatic well testing and PIP calculations using Smart rod pump controllers. Paper SPE 150885 presented at the North Africa Technical Conference and Exhibition held in Cairo. Egypt. February 20–22, 2012.
- [5] McCoy JN. Liquid level measurement. PE July 1975:62–6.
- [6] ERCB Report 74-S Guide for calculating static bottom-hole pressures using fluid-level recording devices. Calgary (Canada): Energy Resources Conservation Board; November 1974.
- [7] Thomas LK, Hankinson RW, Phillips KA. Determination of acoustic velocities for natural Gas. JPT July 1970:889–95.
- [8] Godbey JK, Dimon CA. The automatic liquid level monitor for pumping wells. JPT August 1977:1019–24.
- [9] Huddleston KL, Podio AL, McCoy JN. Application of portable microcomputers to field interpretation of acoustic well surveys. Paper presented at the 1985 SPE computer Technology Symposium. February 28–March 1, 1985. Lubbock (Texas).
- [10] Podio AL, McCoy JN, Huddleston KL. Automatic pressure buildup data acquisition and interpretation using a microcomputer-based acoustic liquid level instrument. Paper SPE 16228 presented at the SPE production operations Symposium. Oklahoma City, Oklahoma. March 9–11, 1987.
- [11] McCoy JN, Podio AL, Becker D. Improved acoustic liquid level surveys by digital data acquisition, processing and analysis. Proc. 38th annual Southwestern Petroleum short course. Lubbock, Texas. 1991. p. 165–183.
- [12] McCoy JN, Huddleston KL, Podio AL. Data processing and display for Echo sounding data. US Patent 5,117,399; May 1992.